https://doi.org/10.5194/bg-2020-323
Preprint. Discussion started: 8 September 2020

Biogeosciences Discussions

Unravelling the physical and physiological basis for the solar-induced chlorophyll fluorescence and photosynthesis relationship

Peiqi Yang[1], Christiaan van der Tol[1], Petya K. E. Campbell[23], Elizabeth M. Middleton[4]

[1]Faculty of Geo-Information Science and Earth Observation (ITC), University of Twente, Enschede, 7500 AE, The Netherlands
[2]Joint Center for Earth Systems Technology (JCET), University of Maryland Baltimore County, Baltimore, MD 21228, USA
[3]Biospheric Sciences Laboratory, NASA Goddard Space and Flight Center, Greenbelt, MD 20771, USA.
[4]Emeritus of Biospheric Sciences Laboratory, NASA Goddard Space and Flight Center, Greenbelt, MD 20771, USA.

Correspondence to: Peiqi Yang (p.yang@utwente.nl)

Abstract. Estimates of the gross terrestrial carbon uptake exhibit large uncertainties. Sun-induced chlorophyll fluorescence (SIF) has an apparent near-linear relationship with gross primary production (GPP). This relationship will potentially facilitate the monitoring of photosynthesis from space. However, the exact mechanistic connection between SIF and GPP is still not clear. To explore the physical and physiological basis for their relationship, we used a unique dataset comprising continuous field measurements of leaf and canopy fluorescence and photosynthesis of corn over a growing season. We found that, at canopy scale, the positive relationship between SIF and GPP was dominated by absorbed photosynthetically active radiation (APAR), which was equally affected by variations in incoming radiation and changes in canopy structure. After statistically controlling these underlying physical effects, the remaining correlation between far-red SIF and GPP due solely to the functional link between fluorescence and photosynthesis at the photochemical level was much weaker. Active leaf-level fluorescence measurements revealed a moderate correlation between the efficiencies of fluorescence emission and photochemistry for sunlit leaves but a weak correlation for shaded leaves. Differentiating sunlit and shaded leaves in the light use efficiency (LUE) models for SIF and GPP facilitates a better understanding of the SIF-GPP relationship at different environmental and canopy conditions. Leaf-level fluorescence measurements also demonstrated that the sustained thermal dissipation efficiency dominated the seasonal energy partitioning while the reversible heat dissipation dominated the diurnal leaf energy partitioning. These diurnal and seasonal variations in heat dissipation underlie, and are thus responsible for, the observed remote sensing-based link between far-red SIF and GPP.

https://doi.org/10.5194/bg-2020-323
Preprint. Discussion started: 8 September 2020


Biogeosciences Discussions

1 Introduction

For our understanding of the Earth's climate, estimates of the gross carbon uptake by terrestrial ecosystems are crucial. Despite considerable progress in measurement systems and models, contemporary estimates of the gross terrestrial carbon uptake still exhibit large uncertainties (Ryu et al., 2019). On the one hand, eddy covariance flux towers provide point measurements at selected locations on all continents, but such *in situ* measurements are sparse. On the other hand, optical remote sensing provides spatially continuous and dense data, but these observations are only indirectly related to the carbon flux. In this respect, the development of sun-induced chlorophyll fluorescence (SIF) measurement techniques from satellites has raised expectations. This is because chlorophyll fluorescence (ChlF) as a by-product of photosynthesis has long been used as a probe of photochemistry in laboratory and field studies (Mohammed et al., 2019). Ever since satellite SIF data products related to the far-red fluorescence peak became available during the past decade, numerous studies have reported a strong correlation between far-red SIF and gross primary production (GPP) at the local, regional and global scales (e.g., Campbell et al., 2019; Damm et al., 2015; Guanter et al., 2014; He et al., 2017; Wieneke et al., 2016). This SIF-GPP link has been employed to estimate photosynthetic capacity (Zhang et al., 2014) and crop yield (Guan et al., 2016).

The rising expectations of far-red SIF rely on a contestable closer relationship with GPP than other optical remote sensing signals, such as well-chosen reflectance indices. In order to make use of SIF quantitatively, it is necessary to understand the physical and physiological meaning of SIF, and to establish mechanistic understanding of its relation to GPP (Gu et al., 2019; Magney et al., 2019; Miao et al., 2018; Yang et al., 2015). In recent studies, the light use efficiency (LUE) model of Monteith (1977) has been the common starting point for describing GPP and SIF as a function of the absorbed photosynthetically active solar radiation (APAR):

$$\mathrm{GPP} = \mathrm{iPAR} \cdot \mathrm{fAPAR} \cdot \Phi_{Pcanopy} \quad (1a),$$

$$\mathrm{SIF} = \mathrm{iPAR} \cdot \mathrm{fAPAR} \cdot \Phi_{Fcanopy} \cdot f_{esc} \quad (1b),$$

where iPAR denotes the available incoming photosynthetically active radiation for a vegetation canopy; fAPAR is the fraction of APAR absorbed by green vegetation; and $\Phi_{Pcanopy}$ and $\Phi_{Fcanopy}$ describe the canopy-scale light use efficiencies for photochemistry and fluorescence, respectively, which are related to the plant physiological status. f_{esc} is the fraction of the emitted far-red fluorescence that escapes the canopy in the viewing direction (per solid angle), which depends on the viewing and illumination geometries and canopy structure (Porcar-Castell et al., 2014; Yang et al., 2020; Yang and Van der Tol, 2018) .

From the LUE model, it is evident that the common terms iPAR and fAPAR are primarily responsible for the often-reported linear relationship between SIF and GPP (Campbell et al., 2019; Dechant et al., 2020; Miao et al., 2018; Rossini et al., 2010;

https://doi.org/10.5194/bg-2020-323
Preprint. Discussion started: 8 September 2020


Biogeosciences Discussions

Yang et al., 2018). The combined contribution of $\Phi_{Fcanopy}$ and f_{esc} to the SIF-GPP relationship is much less clear. It has been argued that $\Phi_{Fcanopy}$ may also contribute to the positive correlation between GPP and far-red SIF, while f_{esc} is viewed as an interfering factor. Guanter et al. (2014) implicitly assumed that a positive relationship between $\Phi_{Fcanopy}$ and $\Phi_{Pcanopy}$ exists and that f_{esc} in the near-infrared region is isotropic and close to unity when explaining the SIF-GPP relationship. However, these assumptions need to be verified, and we still lack a clear conclusion on the physical and physiological basis for the relationship between far-red SIF and GPP.

Dechant et al. (2020) explored the relationship between SIF and GPP for three in situ crop datasets. They found that correcting SIF for canopy scattering (f_{esc}) improved the correlation to APAR but not to GPP. Furthermore, they reported that their estimates of physiological SIF yield ($\Phi_{Fcanopy}$ = SIF/APAR/f_{esc}) showed no clear seasonal patterns and were unlikely to contribute to the positive correlation between GPP and far-red SIF. In contrast, Qiu et al. (2019) reported that the similar correction of SIF for canopy scattering resulted in a better correlation to GPP, and Yang et al. (2020) showed that the estimates of canopy-scale light use efficiency of fluorescence ($\Phi_{Fcanopy}$) were clearly higher in young and mature stages than for the senescent stages, and were correlated with $\Phi_{Pcanopy}$. The inconsistent findings could partly be caused by considerable uncertainties in the estimates of f_{esc} and $\Phi_{Fcanopy}$, especially since the physiological indicators ($\Phi_{Fcanopy}$ and $\Phi_{Pcanopy}$) are still contaminated by canopy structural effects (Yang et al., 2020).

More fundamental understanding can be obtained by returning to the established physiological methods of *in vivo* active fluorescence measurements to discern the relative energy distribution among the four pathways in plants via photosynthesis, fluorescence and heat losses (both sustained and reversible). At the photochemical level in leaves, it is clear that a change in fluorescence emission efficiency can be attributed to a change in the combined efficiencies of photochemistry and heat dissipation, expressed as photochemical quenching (PQ) and non-photochemical quenching (NPQ) of fluorescence (Baker, 2008; Maxwell and Johnson, 2000). The relationship between the photochemical-level photosynthetic light use efficiency (Φ_P) and fluorescence quenching from the maximal level to a steady state was described with the Genty equation (Genty et al., 1989). Semi-empirical generalized relationships have further been developed to model these maximal and steady-state fluorescence levels as a function of photosynthetic light use efficiency and temperature (Rosema et al., 1991; Van Der Tol et al., 2014). However, the universal applicability of the latter models has not been validated, and continuously collected field measurements of active fluorescence at the leaf level along with canopy photosynthesis and SIF measurements are rare, which limits our understanding of their relationship in natural conditions.

The present study aims to assess the drivers of the apparent SIF-GPP relationship using independent measurements of all terms in the light use efficiency model (Eq. 1), collected under different illumination conditions and at different growth stages, at the leaf and canopy levels. We chose a corn crop (*Zea mays* L.), also referred to as maize, because it provides a relatively simple

https://doi.org/10.5194/bg-2020-323
Preprint. Discussion started: 8 September 2020

canopy, typically a row crop with plants nominally having a spherical shape. Maize is also a globally important crop that comprises the "bread-basket" to feed the world. Some have claimed (e.g., Guanter et al., 2014) that the observed far-red SIF obtained from space reveals that the US cornbelt achieves the highest carbon sink of any of Earth's ecosystems. On that basis alone, and because of the importance of agricultural surveys from space for food security reasons, we are justified to conduct a more comprehensive examination of the photosynthetic function and associated fluorescence activity of this crop.

We drew upon a unique dataset comprising growing season-long continuous measurements of a corn crop for leaf active fluorescence, canopy SIF, hyperspectral reflectance, and GPP. With partial correlation analysis we evaluated the contributions of iPAR, fAPAR and APAR to the SIF-GPP relationship at the canopy scale. In parallel, we used active fluorescence measurements to investigate the energy partitioning in leaves to reveal the relationship between fluorescence and photosynthesis at the photochemical level.

2 Materials and methods

2.1 Study site

Field measurements were collected in 2017 at the Optimizing Production inputs for Economic and Environmental Enhancement (OPE^3) field site (De Lannoy et al., 2006) at the US Department of Agriculture's (USDA) Agricultural Research Service (USDA-ARS) in Beltsville, MD, USA (39.0306° N 76.8454° W, UTC-5). The site is instrumented with a 10 m eddy-covariance tower and a height-adjustable tower (i.e., 1.5-4 m tall) supporting the optical spectral measurements and surrounded by corn (*Zea mays* L.) fields. The two towers were located within the same field that was provided the optimal (100%) nitrogen application for this climate zone, separated by approximately 120 m. Three distinct growth phases of the corn canopy were discerned: Young stage (Y) from DOY 192 to 209, Mature stage (M) from DOY 220 to 235 and Senescent stage (S) from DOY 236 to 264.

2.2 Field measurements

The field measurements included active fluorescence observations made on individual leaves, as well as canopy reflectance and SIF retrievals. These were supplemented by crop fluxes and meteorological data from the site's instrumented tower. These measurements cover the 2017 growing season from day-of-year (DOY) 192 to DOY 264, except for the period from DOY 210 to DOY 219. The main field measurements used in this study are listed in Table 1. In what follows, we briefly introduce the measurements used in the present study (the field campaign was described in detail in Campbell et al., 2019).

[Insert Table 1 here]

The site's eddy covariance tower-based system provided 30-minute GPP fluxes continuously collected throughout the growing season. An infrared gas analyzer (Model LI-7200, LI-COR Inc., Lincoln, NE, USA) measured net ecosystem productivity

https://doi.org/10.5194/bg-2020-323
Preprint. Discussion started: 8 September 2020

(NEP), which was further partitioned into GPP and ecosystem respiration (R_e) using a standard approach (Reichstein et al., 2005) which extrapolated nighttime values of R_e into daytime values using air temperature measurements.

Canopy spectral measurements were collected by using a field spectroscopy system, the FLoX (JB Hyperspectral Devices UG, Germany), between 7:00 and 20:00 (local time) with a time sampling interval from 1-3 minutes. The system consists of two spectrometers: a QEpro spectrometer (Ocean Optics, Dunedin, FL, USA) and a FLAME-S spectrometer (Ocean Optics, Dunedin, FL, USA). The QEpro measured down-welling irradiance and up-welling radiance with a 0.3 nm spectral resolution at Full Width at Half Maximum (FWHM) between 650 and 800 nm, which were used to retrieve SIF. The FLAME-S measured the same up-welling and down-welling fluxes but between 400 to 1000 nm with a lower spectral resolution (FWHM of 1.5 nm), which were used to compute canopy values for reflectance (R) and to estimate incident PAR ($iPAR_{canopy}$) and $fAPAR_{canopy}$.

Leaf fAPAR ($fAPAR_{leaf}$) was measured on six days spaced across the growing season (n= 18 samples per day). The leaf absorptance spectra between 350 and 2500 nm for nine leaves were measured in the laboratory with an ASD FieldSpec 4 spectrometer (Malvern Panalytical, Longmont, CO, USA) and an ASD halogen light source coupled with an integrating sphere. The mean $fAPAR_{leaf}$ values per date were computed: 0.92 ± 0.007 (i.e., mean ± stdv) on DOY 192; 0.92 ± 0.01 on DOY 199; 0.91 ± 0.01 on DOY 221; 0.90 ± 0.03 on DOY 222; 0.82 ± 0.03 on DOY 240; and 0.75 ± 0.05 on DOY 263. Finally, $fAPAR_{leaf}$ on the rest of the days was linearly interpolated from those measurements. Therefore, $fAPAR_{leaf}$ values ranged from 0.93 to 0.70 across the growing season.

Leaf-level active fluorescence measurements were collected by using an automated MoniPAM fluorometer system (Walz, Germany) and five MoniPAM emitter-detector probes, which were operated using a MoniPAM Data Acquisition system (Porcar-Castell et al., 2008). Three probes were positioned to measure sunlit leaves in the upper canopy and the remaining two probes collected measurements on shaded leaves within the lower canopy. The fluorometer collected continuous steady state fluorescence (F_s) and maximal fluorescence (F_m) every 10 minutes during the day and night. The MoniPAM measured chlorophyll fluorescence induced by an internal, artificial light source, which produces modulated light with constant intensity (Baker, 2008; Schreiber et al., 1986). In addition to leaf fluorescence measurements, the MoniPAM also measured leaf temperature by an internal temperature sensor and incident PAR ($iPAR_{leaf}$) by a PAR quantum sensor. Leaf APAR ($APAR_{leaf}$) was computed as the product of iPARleaf and $fAPAR_{leaf}$.

2.3 Data quality control and sampling

Data quality control of canopy reflectance, SIF and GPP measurements was conducted prior to the analysis. First, measurements collected on 29 rainy or densely clouded days were excluded. Second, a window-based outlier detection was applied to incident PAR data collected by the FLoX to identify unrealistic short-term fluctuations in atmospheric conditions leading to unreliable SIF retrievals. The fluctuations were detected by finding the iPARcanopy measurements that were not

https://doi.org/10.5194/bg-2020-323
Preprint. Discussion started: 8 September 2020

within ± 3 times the standard deviation for the mean of seven consecutive measurements. Once all cases with fluctuating atmospheric conditions were identified, the reflectance, GPP and SIF measurements acquired within ±half hour of their occurrence were excluded from the analysis. Finally, the remaining FLoX measurements were re-sampled into the 30-minute temporal resolution of the eddy covariance measurements.

2.4 Calculation of canopy SIF, fAPAR and APAR

The QEpro spectral measurements were used to compute Top-of-Canopy (TOC) SIF in the O_2-A absorption feature at around 760 nm (F_{760}). SIF was retrieved using the spectral fitting method (SFM) described in Cogliati et al. (2015). Canopy iPAR ($iPAR_{canopy}$) was computed from the irradiance spectra collected with the FLAME-S spectrometer as the integral of irradiance over the spectral region from 400 to 700 nm. Canopy fAPAR was approximated by using the Rededge NDVI (Normalized Difference Vegetation Index) (Viña and Gitelson, 2005):

$$\mathrm{fAPAR} = 1.37 \cdot \mathrm{RededgeNDVI} - 0.17 \quad (2a),$$

where

$$\mathrm{RededgeNDVI} = \frac{R_{750}-R_{705}}{R_{750}+R_{705}} \quad (2b),$$

where reflectance at specific wavelengths is utilized (R_λ:705 and 750 nm). Rededge NDVI is a widely used index for estimating fAPAR, and Viña and Gitelson (2005) suggest it as an optimal index for fAPAR among various other vegetation indices in corn canopies. We, however, have tested several other indices for estimating fAPAR, including the enhanced vegetation index (EVI) (Huete et al., 2002; Xiao et al., 2004) and the green NDVI (Viña and Gitelson, 2005), and found that the choice among the three indices had little impact on the results in section 3.1.

2.5 Quantifying energy partitioning from leaf fluorescence measurements

The continuous MoniPAM measurements offered a way for assessing the dynamics of energy partitioning in photosystem II (PSII). The pathways include photochemistry (P), fluorescence emission (F) and heat dissipation (H). H is further categorized as a sustained thermal dissipation (D) and a reversible energy-dependent heat dissipation (N). N is controlled by mechanisms that regulate the electron transport of the photosystems and is related to photo-protection mechanisms and NPQ (Baker, 2008).

Relative fluorescence emission efficiency (Φ_F^*) was derived from the MoniPAM steady state fluorescence measurements F_s with a correction for time-varying leaf absorption in the growing season. The correction is needed because F_s responds to the absorbed measurement light rather than the incident measurement light:

$$\Phi_F^* = \frac{Fs}{\mathrm{fAPAR_{leaf}}} \quad (3)$$

MoniPAM maximal fluorescence measurements (F_m), together with the steady state fluorescence (F_s), allows the assessment of the absolute efficiencies of absorbed light energy for photochemistry (Φ_P) and the reversible energy-dependent heat

https://doi.org/10.5194/bg-2020-323
Preprint. Discussion started: 8 September 2020


Biogeosciences Discussions Open Access EGU

dissipation (Φ_N) of PSII. The usual approach to obtain Φ_P is to 'switch off' photochemistry by applying a saturating light to leaves, so that the fluorescence measurements in the presence and absence of photochemistry (F_s and F_m), can be estimated (Maxwell and Johnson, 2000). A generic expression of Φ_P proposed by Genty et al. (1989) was used:

$$\Phi_P = 1 - \frac{Fs}{Fm} \quad (4)$$

Unlike photochemistry, it is difficult to fully inhibit heat dissipation. Nevertheless, long duration dark-adaptation can reduce reversible heat dissipation to zero. Then, fluorescence measurements acquired in the presence and absence of reversible heat dissipation can be estimated. We took the expression proposed by Hendrickson et al. (2004) for Φ_N:

$$\Phi_N = \frac{F_s}{F_m} - \frac{F_s}{F_m^o} \quad (5)$$

where F_m^o is the highest (or maximal) value obtained for dark-adapted leaf fluorescence measurements in the absence of reversible heat dissipation; the pre-dawn value of F_m is typically used as an estimate of true maximal dark-adapted fluorescence (Maxwell and Johnson, 2000). Alternative expressions of Φ_N can be found in the literature, but they are equivalent and convertible to each other. For example, Eq. 5 can be rewritten as $\Phi_N = (1 - \Phi_P)(1 - \frac{F_m}{F_m^o})$. Furthermore, it can be expressed as a function of a commonly used fluorescence parameter NPQ, which is defined as $\frac{F_m^o}{F_m} - 1$ (Baker, 2008). In that formulation, $\Phi_N = (1 - \Phi_P)\frac{NPQ}{NPQ+1}$.

The expression of the sum of Φ_F and Φ_D (symbolized as Φ_{F+D}) is straightforward, because the sum of the efficiencies of the four pathways (Φ_F, Φ_P, Φ_D and Φ_N) is always unity and $\Phi_{F+D} = 1 - \Phi_N - \Phi_P$, and

$$\Phi_{F+D} = \frac{F_s}{F_m^o} \quad (6)$$

Further separation of Φ_F and Φ_D from Φ_{F+D} is difficult, because neither can be inhibited. However, relative efficiency of the sustained heat dissipation (Φ_D^*) across the growing season can be inferred from the pre-dawn values of F_m (i.e., F_m^o). Because F_m^o was measured during the night in the absence of both reversible heat dissipation and photochemistry, a change in F_m^o must be caused by a change in the sustained heat dissipation. Therefore, we can take the maximal pre-dawn $\Phi_{Fm}^* = \frac{F_m^o}{\mathrm{fAPAR_{leaf}}}$, (when Φ_D^* is minimal) as a reference and express Φ_D^* across the growing season as:

$$\Phi_D^* = 1 - \frac{F_m^o / \mathrm{fAPAR_{leaf}}}{\max_{192 \le DOY \le 264}[F_m^o / \mathrm{fAPAR_{leaf}}]} \quad (7)$$

Photosynthetic light use efficiency can be predicted as a function of leaf temperature, ambient radiation levels, intercellular CO_2 concentrations C_i, and other leaf physiological parameters (e.g., photosynthetic pathways, maximum carboxylation rate

https://doi.org/10.5194/bg-2020-323
Preprint. Discussion started: 8 September 2020


Biogeosciences Discussions Open Access EGU

V_{cmo}) by using a conventional photosynthesis model of Collatz et al., (1992; 1991). Van der Tol et al., (2014) established empirical relationships between fluorescence emission efficiency and photosynthetic light use efficiency under various environmental conditions by using active fluorescence measurements. With these relationships, the fraction of the absorbed radiation by a leaf emitted as fluorescence and dissipated as heat can be simulated. The MoniPAM system measured leaf temperature and incoming radiation intensity. We reproduced the efficiencies of photochemistry, fluorescence, and reversible and sustained heat dissipation by using the biochemical model of Van der Tol et al., (2014). The field measurements of leaf temperature and incoming radiation intensity were used for the model input. We set V_{cmo} to 30 μmol m^{-2} s^{-1}, which is a recommended value for C4 crops, and the rest of the model parameters (e.g., C_i) to their default values. In this way, we simulated the efficiencies for the temporal resolution of the MONIPAM measurements (i.e., 10 minutes) and examined the relationship among the efficiencies as predicted by the biochemical model.

2.6 Statistical analysis

Pearson correlation coefficients (ρ) were computed to evaluate the relationships between pairs of observations, such as Φ_P and Φ_F^*, or GPP and SIF. In addition to the correlation coefficients, partial correlation coefficients were computed to measure the degree of association between GPP and SIF, where the effect of a set of controlling variables was removed, including fAPAR, iPAR and APAR. Partial correlation is a commonly used measure for assessing the bivariate correlation of two quantitative variables after eliminating the influence of one or more other variables (Baba et al., 2004). The partial correlation between x and y given a controlling single variable z was computed as

$$\rho_{x,y(z)} = \frac{\rho_{x,y} - \rho_{x,z}\rho_{y,z}}{\sqrt{1-\rho_{x,z}^2}\sqrt{1-\rho_{y,z}^2}} \quad (8)$$

where $\rho_{x,y}$ is the Pearson correlation coefficient between x and y.

Partial correlation can be calculated to any arbitrary order. $\rho_{x,y(z)}$ is a first-order partial correlation coefficient, because it is conditioned solely on one variable (z). We used a similar equation to calculate the second-order partial coefficient that accounts for the correlation between the variables x and y after eliminating the effects of two variables z and q (de la Fuente et al., 2004).

$$\rho_{x,y(zq)} = \frac{\rho_{x,y(z)} - \rho_{x,q(z)}\rho_{y,q(z)}}{\sqrt{1-\rho_{x,q(z)}^2}\sqrt{1-\rho_{y,q(z)}^2}} \quad (9)$$

3 Results

3.1 Relationship between canopy SIF and GPP observations

Fig. 1a confirms the linear SIF-GPP relationship reported in previous studies and shows that F_{760} and GPP were strongly correlated with an overall correlation ρ = 0.83. This correlation was slightly stronger than the relationship between $APAR_{canopy}$

https://doi.org/10.5194/bg-2020-323
Preprint. Discussion started: 8 September 2020


Biogeosciences Discussions Open Access EGU

and GPP (an overall ρ = 0.80, Fig. 1b). The $APAR_{canopy}$-GPP relationship was apparently comprised of parallel groups of responses (colors) with large variation in GPP exhibited for the same levels of $APAR_{canopy}$ (Fig. 1b). This relationship complies with the common understanding of the response of photosynthesis to light showing the well-known saturation with irradiance as photosynthesis of the whole canopy gradually shifts from light limitation to carbon limitation, while the unexplained (by light intensity) variation in GPP can be attributed to stomatal aperture responses and a time-varying carboxylation capacity, especially in the upper sunlit canopy, which experienced larger variations of light intensity. SIF, which is affected by both light and carbon limitations, shows a more linear response to GPP than $APAR_{canopy}$ (Figs. 1a vs. 1b).

[Insert Figure 1 here]

Incoming radiation (i.e., $iPAR_{canopy}$) had a strong, positive linear relationship with SIF, GPP and $APAR_{canopy}$ (as shown in Figs. 1 and 2). We investigated these canopy-scale relationships with partial correlation analysis as diagrammed in Fig. 2, where for simplicity's sake, the subscripts denoting "canopy" variables were omitted in the diagram. Our team (Yang et al., 2020) and others (Miao et al., 2018; Migliavacca et al., 2017) have previously demonstrated that in addition to incoming radiation intensities, the energy available for photochemistry and fluorescence (i.e., $APAR_{canopy}$) is strongly affected by canopy structure and leaf biochemistry. As a result, there were cases of low SIF, GPP and/or $APAR_{canopy}$ values at high $iPAR_{canopy}$ (Fig. 1, red and orange dots), and *vice versa* high SIF, GPP and/or $APAR_{canopy}$ values at low $iPAR_{canopy}$ (Fig. 1, blue and violet dots). This is shown in the correlation diagram as well (Fig. 2) which indicates that SIF, GPP and $APAR_{canopy}$ were all moderately dependent on leaf biochemistry as well as on canopy structure according to their correlations with $fAPAR_{canopy}$, i.e., $\rho_{SIF,fAPAR}$= 0.60, $\rho_{GPP,fAPAR}$= 0.58 and $\rho_{APAR,fAPAR}$= 0.70 (i.e., numbers in bold, blue text, Fig. 2). Compared with either $iPAR_{canopy}$ or $fAPAR_{canopy}$, $APAR_{canopy}$ as their product (located in center, Fig. 2) can better explain the variations in SIF and GPP observations, with Pearson correlations of ρ = 0.92 and 0.80, respectively.

[Insert Figure 2 here]

After removing the effects of this important controlling variable that affects both SIF and GPP, namely $APAR_{canopy}$, the correlation between GPP and SIF was weak ($\rho_{SIF,GPP(APAR)}$= 0.27; refer to results below the triangle's baseline). In contrast, the correlation between SIF and GPP remained significant after controlling for the effects of the components of canopy APAR, either $fAPAR_{canopy}$ or $iPAR_{canopy}$, i.e., $\rho_{SIF,GPP(fAPAR)}$= 0.72, $\rho_{SIF,GPP(iPAR)}$= 0.66 (equations below the triangle, Fig. 2).

We further investigated how the SIF-GPP relationship varied seasonally with growth stage and diurnally with time of the day (Fig. 3). The SIF-GPP correlation was significantly lower (by 22-27%) for the senescent canopy than for the young and mature canopy. The Pearson correlation coefficient was highest when the canopy was fully developed with the underlying surface covered in the mature stage (ρ = 0.77, Fig. 3b). As for the different times of a day, we found that their correlations were the

https://doi.org/10.5194/bg-2020-323
Preprint. Discussion started: 8 September 2020


Biogeosciences Discussions

strongest in the afternoon (ρ = 0.89) while ρ was only 0.76 when the data were acquired in the morning, representing an order of magnitude improvement of 13% from mid-morning to mid-afternoon observations (Figs 3d vs. 3f).

[Insert Figure 3 here]

3.2 Dynamics of energy partitioning in photosystems

The continuously acquired active fluorescence measurements offered a way to assess the dynamics of energy partitioning in photosystems and facilitated the understanding of the relationship between fluorescence and photosynthesis before aggregation to the canopy, at the photochemical level. We investigated how the partitioning evolved over time.

During the nighttime, as can be seen from the responses in the dark-bars in Figs. 4a and 4b, the photosystem energy partitioning was stable for all leaves, whether they were designated as sunlit or shaded during the day. Three efficiencies (Φ_P, Φ_F^* and Φ_D^*) showed little overnight change, and the reversible heat dissipation Φ_N was always close to zero. This null response for Φ_N agrees with the known status/behavior of the most important driver of reversible heat dissipation, the xanthophyll pigment cycle, which reverts overnight to the energy-neutral form violaxanthin, and then converts during the day to antheraxanthin in moderately high light levels and subsequently to zeaxanthin at high light levels by chemical de-epoxidation (Middleton et al., 2016; Müller et al., 2001).

[Insert Figure 4 here]

During the daytime, there were dramatic day-to-day changes in energy partitioning to photochemistry, fluorescence and reversible heat dissipation (Figs. 4a and 4b). Generally, both Φ_F^* and Φ_N increased during mornings to midday and decreased afterwards, except that Φ_N exhibited unexplained midday dips during the senescent stage. On the other hand, Φ_P decreased during mornings to midday lows and increased afterwards (i.e., Φ_P diurnals were bowl-shaped, as shown in many studies). The changes in Φ_N and Φ_P corresponded closely with the changes in incident radiation, while Φ_F^* changes corresponded closely with the dynamics in incident radiation in the morning but not at midday when the radiation level was high.

At the seasonal scale (Fig. 4), however, the nighttime energy partitioning over the three other pathways (Φ_P, Φ_F^* and Φ_D^*) displayed substantial variations. The nighttime Φ_P was about 0.82 on all days during the young and mature stages, which is close to the theoretical maximal value (Zhu et al., 2008), but it was only about 0.64 during the senescent stage. Similarly, the nighttime relative light use efficiency of fluorescence Φ_F^* clearly decreased as the canopy development progressed from the physiologically robust (young and mature) stages to the senescent stage. The seasonal/growth stage decreases during nighttime in both Φ_F^* and Φ_P were attributed to an increase of sustained heat dissipation Φ_D^* since nighttime Φ_N was always close to zero. In extrapolating Φ_D^* to daytime, we assumed that the sustained heat dissipation remained unchanged within any full day

https://doi.org/10.5194/bg-2020-323
Preprint. Discussion started: 8 September 2020


Biogeosciences Discussions Open Access EGU

(from 0:00 to 24:00), but noticeable changes in Φ_D^* sometimes occurred between two consecutive days, e.g., between Φ_D^* on DOY 194 and DOY 195, and between DOY 230 and DOY 231, as indicated in Fig. 4.

It is evident that the contribution to the photosynthetic process by the combined fluorescence and sustained heat dissipation group (Φ_{F+D}, red color in Fig. 5) increased through the growing season, to competitively reduce photochemical efficiency (Φ_P, green color), especially during senescence. Additionally, the reversible heat dissipation (Φ_N, gold color) was generally higher at the senescent stage than at the young and mature stages, which contributed to the reduction in photochemical efficiency as well. In the pie charts, we focus on the energy partitioning in both nighttime and midday since they represent the potential maximal Φ_P (i.e., the photosynthetic reaction centers in the nighttime are mostly open) and the steady-state Φ_P at the most common time of day for satellite observations, respectively.

[Insert Figure 5 here]

The pie charts (Fig. 5) clearly show how these relative efficiency pathway contributions changed with growth stage. The nighttime Φ_P was reduced by 17% between the young and senescent stages, while Φ_{F+D} increased by 16% during senescence. The pie charts also clearly show the very strong role of reversible heat dissipation in limiting midday photosynthesis throughout the growing season. For example, the per cent contribution for the pathways from the young crop (DOY 196) was 33% for Φ_P, 22% for Φ_N, and 45% for Φ_{F+D}). The corresponding values for leaves in the mature crop (DOY 232) were 30%, 12%, and 59%. And for the leaves in the senescing crop (DOY 254), the corresponding values were 13%, 26%, and 61%. Combining these together, Fig. 5 further highlights the complexity of energy efficiency dynamics underlying the photosynthetic process.

3.3 Relationships among photosynthesis, fluorescence and heat dissipation at leaf level

Next, we examine the leaf-level efficiency terms obtained from *in situ* measurements, in terms of their combined responses. The first set compares Φ_F^* and Φ_P, in the context of variable $iPAR_{leaf}$ (Figs. 6a, b). This figure clearly shows that the relationship between Φ_F^* and Φ_P during daylight (9:00 - 17:00) was different for the sunlit (sun adapted) vs. shaded (shade adapted) leaves, since the sunlit leaves were more often exposed to iPAR above 1000 μmol m^{-2} s^{-1}. The higher Φ_P values were obtained for relatively low $iPAR_{leaf}$, whether sunlit or shaded. For sunlit leaves, Φ_F^* and Φ_P were positively correlated overall (ρ = 0.53, Fig. 6a) and in conditions with moderate to high light intensity ($iPAR_{leaf}$ >500 μmol m^{-2} s^{-1}, excluding blue and teal colored dots), ρ = 0.60. In contrast, at low light intensity ($iPAR_{leaf}$ <500 μmol m^{-2} s^{-1}, blue dots), correlation between Φ_F^* and Φ_P was weak and negative for Φ_P>0.4. These two efficiency terms were uncorrelated in shaded leaves (Fig. 6b), and Φ_F^* was much lower in the shaded than in sunlit leaves.

[Insert Figure 6 here]

https://doi.org/10.5194/bg-2020-323
Preprint. Discussion started: 8 September 2020


Biogeosciences Discussions Open Access EGU

At the seasonal scale, the midday Φ_F^* and Φ_P values (the average of all values acquired between 11:00 and 14:00) had a quasi-linear, positive relationship for both the sunlit and shaded leaves when $iPAR_{leaf}$ >500 µmol m^{-2} s^{-1} (Fig. 6c). In contrast, at low average midday light intensities, the relationships were clearly negative. The Φ_P values tended to decrease with the increasing light intensities while the relationship between Φ_F^* and $iPAR_{leaf}$ was not definite. However, the seasonally averaged ranges for Φ_F^* in sunlit and shaded leaves clearly represent two populations: Φ_F^* shaded was < 110 (Fig. 6b) whereas Φ_F^* sunlit > 100 (Fig. 6a). These results could have implications for interpreting canopy-scale measurements.

The relationship obtained between Φ_P and Φ_N was considerably stronger for both sunlit and shaded leaves (Figs. 7a, b) than the correlation between Φ_F^* and Φ_P previously shown for sunlit leaves (Fig. 7a). Here, both sunlit and shaded leaves showed consistent and strong linear decreases in Φ_P as Φ_N increased in response to variations in the intensity of incoming light ($iPAR_{leaf}$) (Figs. 7a, b). Furthermore, the Φ_P and Φ_N relationships definitely varied in response to the sustained heat dissipation (Φ_D^*, levels represented in the color bar) in a similar fashion for both sunlit and shaded leaves, although higher Φ_D^* values (orange and red dots) were obtained in sunlit leaves. The efficiency of photochemistry obviously declined at higher Φ_D^*, as indicated with the arrows in Fig. 7, especially pronounced in sunlit leaves. When both thermal dissipations were strongly expressed, the Φ_P was greatly reduced; in sunlit leaves, this reduction was ~40%.

[Insert Figure 7 here]

At the seasonal scale, as can be seen from Figs. 4 and 5, Φ_P decreased while Φ_D^* increased as the canopy progressed through its growth stages. Their seasonal relationship is depicted in Fig. 7c, showing a same-day comparison of the midday Φ_P value (the average between 11:00 and 14:00), as a function of Φ_N across the growing season noting that Φ_D^* remained unchanged within any full day. Generally, Φ_N and Φ_P exhibited an overall negative correlation, but clearly their relationship was regulated by Φ_D. This is seen in the different midday Φ_P responses at high vs. low Φ_D^* values. At the same level of Φ_N, the magnitudes of midday Φ_P varied by up to 0.45 (65%) due to variations in the efficiency of the sustained heat dissipation which varied between 0.1 and 0.6.

We have shown that Φ_P was regulated by heat dissipation (Figs. 5 and 7), and was moderately correlated with Φ_F^* for the sunlit leaves (Fig. 6). With the dynamics of energy partitioning within the photosystem now quantified, we interpret the emerging relationship between photochemical and fluorescence efficiencies, namely Φ_P and Φ_F^* (Table 2), in the context of thermal dissipation efficiencies (Φ_N, Φ_D^*). After eliminating the effects of both sustained and reversible heat dissipation, Φ_P and Φ_F^* were negatively and equally correlated (ρ = -0.75) for both sunlit and shaded leaves. As surprising as this is, the presence of either sustained or reversible heat dissipations changed this underlying negative relationship (Φ_P vs. Φ_F^*) into an observed apparent positive relationship at leaf scale, which contributes to the positive relationship of GPP and SIF at canopy scale. In fact, accounting for the effects of either Φ_N or Φ_D^* reduced the correlation coefficients between Φ_P and Φ_F^*. For sunlit leaves,

https://doi.org/10.5194/bg-2020-323
Preprint. Discussion started: 8 September 2020

controlling for only Φ_N reduced the correlation from 0.53 to 0.05 (by ~0.48 units); after controlling for only Φ_D^*, the correlation dropped by 0.45 units to 0.08. For shaded leaves this reduction was from 0.10 to -0.31 after controlling for Φ_N, or to -0.35 after controlling for Φ_D^*. These results represent trends that include both diurnal and seasonal variations.

[Insert Table 2 here]

Results of model simulations are presented in Figs 8 and 9. In comparison with Figs. 6 and 7 that describe our *in situ* measurements, these two figures show that the biochemical model outputs were more successful in describing photosynthetic efficiency as a function of reversible heat dissipation (Φ_N) than fluorescence efficiency (Φ_F). Specifically, for the Φ_P-Φ_F relationships, the Fig. 8 simulation shows some similarity to the Fig. 6 measurements, but clearly does not capture the different responses we obtained for sunlit versus shaded leaves. However, Fig. 9 does generally replicate the general responses expected based on in situ measurements (Fig. 7), portraying the strong negative impact of Φ_N on Φ_P, but it doesn't convey the variability captured under field conditions. These differences occurred in the simulations because we did not consider the physiological (i.e., enzyme activity) or physical (i.e., thickness, pigment ratios) differences among leaves at different growth stages. Neither did we consider the physical differences or photochemical potential differences (e.g., total chlorophyll content and Chl a/b ratios; rubisco activity) between sunlit and shaded leaves in this modelling experiment. Therefore, it is to be expected that the simulations for sunlit and shaded leaves would be similar, and not displaying the differences observed in field measurements. Furthermore, we did not include changes in leaf display geometry induced by low water stress (i.e., drought), a common phenomenon in corn plants, in either measurements or simulations. Another likely reason contributing to the differences between simulations and observations is that in using the model of Van der Tol et al. (2014) to derive Φ_F from Φ_P, Φ_D is assumed to be a constant and Φ_N is empirically estimated as a function of Φ_P/Φ_{P0}. The observations shown in Figs. 4 and 5 prove that Φ_D varied over the growing season, and therefore, cannot be considered as a constant. These findings may help improve the modelling of Φ_F at the biochemical level and thus improve our understanding of the relationship between SIF and GPP at the canopy scale.

[Insert Figure 8 here]

[Insert Figure 9 here]

3.4 Comparison of light use efficiencies at leaf and canopy levels

The responses of the efficiencies to APAR and the relationships between these efficiencies are diagrammed in Fig. 10, showing the Pearson correlation coefficients between pairs of variables, for leaves (Fig. 10a) that were either sunlit or shaded (indicated in bold, blue text), and for canopy (Fig. 10b).

[Insert Figure 10 here]

https://doi.org/10.5194/bg-2020-323
Preprint. Discussion started: 8 September 2020

At the leaf level, we see that Φ_F^* showed moderate correlation to Φ_P for sunlit leaves (ρ = 0.53) but very low correlation to Φ_P for shaded leaves (ρ = 0.10). The highest correlations were negative, denoting inverse relationships between Φ_N and Φ_P (-0.74 sunlit and -0.87 shaded), whereas similar positive correlations (0.64 sunlit and 0.68 shaded) were obtained between Φ_N and $APAR_{leaf}$ (located in center, Fig. 10a), as expected since Φ_N is well known to be light-level sensitive when invoking the xanthophyll cycle. Notice that all of the high correlations (>0.64 or <-0.74), whether positive or negative, are located on the left-hand side of Fig. 10a, which compares efficiencies of photochemistry with efficiencies of reversible thermal dissipation (Φ_N) and their connection through $APAR_{leaf}$. The remaining correlations on the right-hand side, between Φ_F^* and either Φ_P, Φ_N, or $APAR_{leaf}$, are significantly lower (from -0.33 to 0.53).

At the canopy level, $\Phi_{Fcanopy}$ also showed moderate correlation to $\Phi_{Pcanopy}$ with ρ = 0.37 (Fig. 10b), which falls between the values for sunlit and shaded leaves (Fig. 10a). An inverse relationship between $\Phi_{Pcanopy}$ and $APAR_{canopy}$ (-0.41) was found at the canopy level, but this correlation was much weaker than that at the leaf level (-0.75 for both sunlit and shaded leaves). The photochemical reflectance index PRI= $\frac{R_{531}-R_{570}}{R_{531}+R_{570}}$ (Gamon et al., 1992), as an indicator of $\Phi_{Ncanopy}$, appeared to have no correlations with either $APAR_{canopy}$ or $\Phi_{Pcanopy}$, while at the leaf level these three variables had strong correlations (located on the left-hand side of Fig. 10a). Comparing the efficiencies obtained from the leaf- and canopy-level measurements (i.e., $\Phi_{Pcanopy}$vs. Φ_P or $\Phi_{Fcanopy}$vs. Φ_F^*), no clear relationships were found (ρ <0.1, data not shown).

4 Discussion

4.1 Physical basis for the SIF-GPP relationship

Incoming radiation intensity, leaf biochemistry, leaf and canopy structure all affect $APAR_{canopy}$, the energy source for photosynthesis, SIF and heat dissipation. We found an equal contribution of $iPAR_{canopy}$ and $fAPAR_{canopy}$ to the observed SIF-GPP canopy relationship. The correlation coefficients between SIF and GPP remained relatively high after controlling either term. In stark contrast, after holding APAR (their product, $iPAR_{canopy}$ x $fAPAR_{canopy}$) constant, the SIF-GPP canopy correlation coefficient was reduced from 0.83 to 0.27. This demonstrates the dominance of $APAR_{canopy}$ in determining the relationship between SIF and GPP. Compared to $APAR_{canopy}$, SIF was slightly better correlated with GPP (Fig. 1). The physiological information implied in GPP was seemingly better expressed with SIF than $APAR_{canopy}$.

The interfering effects of f_{esc} at canopy scale have not been considered explicitly. They are implicit in the relations of $\rho_{SIF,GPP(APAR)}$ (Qiu et al., 2019). When accounted for, they may provide a better estimate of the correlation attributable to the physiological response of photosystems (i.e., $\rho_{SIF,GPP(APAR,fesc)}$ > 0.27). The magnitude and sign of $\rho_{SIF,GPP(APAR)}$ are nevertheless consistent with the moderate correlation we found between leaf Φ_F^* and Φ_P for sunlit leaves and the weak

https://doi.org/10.5194/bg-2020-323
Preprint. Discussion started: 8 September 2020

correlation for shaded leaves (Figs. 6 and 10a). In addition, we found that the positive relationship between Φ_F^* and Φ_P at the seasonal time scale is dominated by the progressive increase of sustained heat dissipation (Φ_D^*) during senescence. In contrast, there was significant diurnal but no clear seasonal variation of Φ_N.

4.2 Physiological basis for the SIF-GPP relationship

Clear differences between the responses of sunlit and shaded leaves influence the correlation for the canopy as a whole. The Φ_F and Φ_P of sunlit leaves exposed to moderate or high $iPAR_{canopy}$ exhibited a moderately strong linear relationship, while no such relationship existed for leaves at low $iPAR_{canopy}$ (independent of whether the leaves were classified as sunlit or shaded leaves). Leaves regularly receiving sunlight during development (sunlit leaves) differ structurally and biochemically from leaves in lower light positions in the canopy. Shaded leaves are often thinner, smoother, and larger in surface area (Dai et al., 2004). The larger shaded leaves provide a larger area for absorbing light energy for photosynthesis where light levels are lower. In contrast, smaller sunlit leaves provide less surface area for the loss of water through transpiration which is higher due to direct exposure to solar radiation. The greater mesophyll thickness of sunlit leaves produces more inter-cellular spaces to facilitate increased carbon dioxide conductance into their smaller chloroplasts, producing greater rates of photosynthesis per leaf unit area in sunlit leaves (Givnish, 1988; Jackson, 1967).

Compared to the relationship between fluorescence emission efficiency, total heat dissipation (both D and N) provided a robust and direct indicator of photosynthetic light use efficiency (Fig. 7). Reversible heat dissipation is the main regulating mechanism for the dissipation of photosynthetic energy, and is responsible for the positive relationship between Φ_F and Φ_P at diurnal scales, though less so at seasonal scales when sustained heat dissipation is dominant (Heber et al., 2006). Remote sensing monitoring at the canopy/landscape scale of the reversible efficiency of heat dissipation is still challenging. It is well known that changes in Φ_N are often associated with changes in leaf green reflectance due to changes in the de-epoxidation state (DEPS) of xanthophyll cycle pigments. The photochemical reflectance index (PRI) utilized the link between the biochemical changes within xanthophyll cycle expressed with a narrow-band green reflectance, providing a way to remotely assess photosynthetic light use efficiency (Gamon et al., 1992; Garbulsky et al., 2011), but the link becomes partially obscured at canopy scale due to the effects of canopy structure and sun-observer geometry (Hilker et al., 2009; Middleton et al., 2009). Because of these interfering effects, canopy PRI showed very weak overall relationship with $APAR_{canopy}$ (ρ=0.28, Fig. 10b), which clearly differed from the connection between Φ_N and $APAR_{leaf}$ at the leaf level ($\rho \geq 0.64$, Fig. 10a).

Since the reversible heat dissipation pathway is such a strong competitor to photochemistry, especially in the sunlit canopy fraction, it seems very important to fully understand the green reflectance link to the energy regulation via the xanthophyll cycle, and then develop radiative transfer modelling approaches to translate this link to the canopy level. In this regard, Vilfan et al. (2018) extended the Fluspect leaf radiative transfer model to simulate xanthophyll driven leaf reflectance dynamics.

https://doi.org/10.5194/bg-2020-323
Preprint. Discussion started: 8 September 2020


Biogeosciences Discussions

Further efforts on implementing this extended model in canopy radiative transfer models will connect efficiencies of photochemistry and reversible heat dissipation to canopy reflectance observations. This may open new opportunities to estimate photosynthetic light use efficiency and improve GPP estimation using remote sensing methods *in situ* and from space.

4.3 Physically and physiologically joint effects on the SIF-GPP relationship

The canopy equivalent efficiencies ($\Phi_{Fcanopy}$ and $\Phi_{Pcanopy}$) are composed of integrals of the efficiencies of leaves of the sunlit and shaded canopy fractions. The correlation between the canopy effective equivalents of Φ_F and Φ_P may be expected to take a value between the equivalent correlation of leaf-level Φ_F and Φ_P for sunlit leaves (ρ = 0.53) and for shaded leaves (ρ = 0.10). This means that the ability to view the SIF and reflectance hot spots (whether they occur together or not) from sunlit leaves varies with viewing angle and time of day (e.g., illumination angle, diffuse light). We suggest that these factors strongly affect f_{esc}. Therefore, they must, in turn, affect the success of remote sensing relationships for SIF-GPP (Yang and Van der Tol, 2018). Likewise, these factors also affect the variability of the APAR-GPP relationship (Dechant et al., 2020; Qiu et al., 2019), and the LUE-GPP relationship (e.g., Middleton et al., 2019).

The exact correlation between $\Phi_{Fcanopy}$ and $\Phi_{Pcanopy}$ at canopy scales depends on both the relative contributions of sunlit and shaded leaves to the canopy equivalents and the native correlation of the efficiencies at leaf level (Köhler et al., 2018; Mohammed et al., 2019). Canopy structure dictates the relative abundance and thus the relative weights of these contributing factors to the canopy equivalent Φ_F and Φ_P. The weight is not only determined by leaf class abundance, but also by the relative magnitude of the SIF and GPP response of the leaf classes. Sunlit leaves during daytime usually constitute a greater contribution to the effective canopy efficiencies than shaded leaves, simply because sunlit leaves tend to emit a higher SIF signal and, at the same time, produce a higher GPP. This suggests that the correlation between the canopy effective equivalents of Φ_F and $\Phi_P$tends to be closer to the correlations of leaf-level Φ_F and $\Phi_P$for sunlit leaves (ρ =0.53) than for shaded leaves.

The LUE models as shown in Eq. 1 are, essentially, one-big-leaf models. The one-big-leaf approach assumes that canopy photosynthesis or SIF have the same relative responses to the environment as any single leaf, and that the scaling from leaf to canopy is therefore linear (Friend, 2001). However, sunlit and shaded leaves clearly showed a different Φ_F-$\Phi_P$relationship (Figs. 6 and 10). In order to better interpret the SIF-GPP relationship, we recommend a revision of the LUE model of SIF and GPP (Eq. 1) by separating the contributions of sunlit and shaded leaves:

$$\mathrm{GPP} = \sum_{\mathrm{n=sunlit,shaded}} \mathrm{iPAR} \cdot \mathrm{fAPAR}^{\mathrm{n}} \cdot \Phi_P^{\mathrm{n}} \quad (10a),$$

$$\mathrm{SIF} = \sum_{\mathrm{n=sunlit,shaded}} \mathrm{iPAR} \cdot \mathrm{fAPAR}^{\mathrm{n}} \cdot \Phi_F^{\mathrm{n}} \cdot f_{esc}^{\mathrm{n}} \quad (10b),$$

https://doi.org/10.5194/bg-2020-323
Preprint. Discussion started: 8 September 2020

This approach updates the existing one-big-leaf LUE models into two-big-leaf LUE models. The idea of differentiating sunlit and shaded leaves in vegetation modelling has been applied in predicting canopy temperature and photosynthesis, and was shown for the canopy PRI response when including both sunlit and shaded leaves in model simulations of field results (Dai et al., 2004; Luo et al., 2018; Wang and Leuning, 1998; Zhang et al., 2017), but has not been implemented in the LUE model for SIF. More explicit models, such as SCOPE (Soil-Canopy-Observation of Photosynthesis and Energy fluxes, Van Der Tol et al., 2009), consider more classes of leaves with varying ambient temperature and radiation levels, but they require many parameters as input. The two-big-leaf LUE models consider the major difference of leaves in a canopy, and are relatively simpler compared with SCOPE but more realistic compared with one-big-leaf LUE models in linking SIF and GPP.

The fraction of sunlit canopy is determined by canopy structure and the direction of incoming light as well as the fraction of diffuse light. Hence, it is expected that these factors will affect the contribution of sunlit and shaded leaves to the canopy SIF-GPP correlation. Furthermore, the instantaneous sun-view angle geometry affects where the sunlit leaves occur during the day and the likelihood of their being viewed at particular angles (e.g., nadir). This means that the ability to view the SIF hot spot emitted from sunlit leaves varies with viewing angle and time of day. We suggest that these factors strongly affect f_{esc} which must, in turn, affect the SIF-GPP remote sensing relationship (Yang and Van der Tol, 2018).

Intuitively, in fully contiguous vegetation canopies the leaves in the upper layer (which are often sunlit) contribute a major fraction to the whole canopy of APAR, whereas $fAPAR_{shaded}$ is small. Therefore, Φ_F^{sunlit} and Φ_P^{sunlit} have much larger relative contributions to $\Phi_{Fcanopy}$ and $\Phi_{Pcanopy}$, respectively. Hence, a stronger relationship between SIF and GPP for dense canopies is expected since Φ_F^{sunlit} and Φ_P^{sunlit} are moderately correlated. This insight can provide some explanation for the seasonally varying results describing canopy SIF and GPP (Fig. 3 a-c), where the SIF-GPP relationship varied with the growth stages: for the Young crop (ρ= 0.72); Mature crop (ρ = 0.77); and the Senescent crop (ρ = 0.50).

Furthermore, the effects of diffuse light (the diffuse/direct iPAR ratio) on the relationship between SIF and GPP can be explained by the revised equation (Eq. 10). When the fraction of diffuse light is higher (e.g., a hazy, or cloudy day), there is greater iPAR penetration into lower canopy layers (the shaded leaves). As a result, $fAPAR_{shaded}$ increases while $fAPAR_{sunlit}$ decreases. This leads to a higher contribution of shaded leaves to the SIF-GPP relationship at canopy level, and weakens the SIF-GPP correlation. This was indeed observed in earlier field measurements reported in Miao et al. (2018), which showed that both the SIF-GPP correlation and the correlation between the SIF/APAR and GPP/APAR ratios were significantly weaker under cloudy conditions than sunny conditions. The relative fraction of diffuse light is also a possible cause for the diurnally varying correlation between SIF and GPP (Fig. 3 d-f), where the SIF-GPP relationship varied at different times of day: for the data acquired in the morning (ρ = 0.76); for the data acquired in the midday (ρ = 0.83); and for the data acquired in the afternoon (ρ = 0.89). This highlights the unique physiological information of SIF for monitoring GPP, and the joint effects of

https://doi.org/10.5194/bg-2020-323
Preprint. Discussion started: 8 September 2020

535 incoming radiation, canopy structure and leaf physiology on the SIF-GPP relationship. We suggest that the canopy structure, illumination and viewing conditions, and especially the foliage thermal dissipation must be taken into account to accurately represent the physiological underpinnings of the observed SIF-GPP relationships.

A simple model was used to examine the sensitivity of the fraction of sunlit canopy to LAI, leaf angle distribution function
540 (LIDF) and solar zenith angles (θ_s). Considering a vegetation canopy as a turbid medium consisting of leaves, the instantaneous sunlit fraction can be estimated as a function of the direction of incoming light, canopy LAI (L) and leaf angle distribution. In stochastic models describing the transfer of radiation in plant canopies, the probability of the leaves being sunlit at a specified vertical height x (i.e., x= 0 referring to top of canopy, x= -1 referring to bottom of canopy) can be estimated as $P_s = \exp(kLx)$, where L is canopy LAI and k the extinction coefficient, which is determined by the solar direction and leaf angle distribution
545 (He et al., 2017; Stenberg and Manninen, 2015). The computation of k is explicitly given in Verhoef (1984) by projecting the leaf area into the direction of the sun. In the model SCOPE (Van Der Tol et al., 2009), the total fraction of sunlit canopy LAI is the integral of P_s in the vertical direction given as:

$$P_{sun} = \frac{1}{kL}(1 - \exp(-kL)) \quad (11)$$

550 The effects of LAI, leaf angle distribution function (LIDF) and solar zenith angles (θ_s) on the instantaneous sunlit canopy fraction are presented in Fig. 11. In line with our intuitive understanding, the fraction of sunlit canopy decreases with increasing canopy LAI in denser canopies. This fraction also decreases with increasing solar zenith angle, which are also affected by the leaf angle distribution. The important quantity for our purposes is the relative (not absolute) angular difference between the sun and leaf positions.

555 ***[Insert Figure 11 here]***

A limitation of the current SCOPE capability for describing physiological responses is related to capturing the changing light environments that affect estimates of the sunlit/shaded fractions. This is because SCOPE and most radiative transfer models for vegetation assume steady state conditions and lack temporal memory of state variables at different times. SCOPE predicts
560 the sunlit/shaded fractions at one moment while the shaded and sunlit leaves discussed in this paper are a result of long-term adaption to the light conditions (i.e., sun-adapted and shade-adapted leaves). Nevertheless, we can gain insights into relationships under specified conditions, which can serve as new information to be used in updating the models.

5 Conclusions

We have used a unique dataset to explore the relationship between fluorescence and photosynthesis at leaf and canopy levels
565 over a growing season in a corn canopy. We have quantified the contribution of incoming radiation, canopy structure and plant physiology to the SIF-GPP relationship by using partial correlation analysis.

https://doi.org/10.5194/bg-2020-323
Preprint. Discussion started: 8 September 2020

We demonstrate that the observed positive relationship between SIF and GPP is largely due to the fact that both of them are dependent on APAR (i.e., not on iPAR). Incoming radiation and canopy structure had comparable contributions to the SIF-GPP relationship. After eliminating the effects of variable APAR on the SIF-GPP relationship, the apparent positive relationship between SIF and GPP became much weaker. However, there is still some remaining connection due to the functional link between fluorescence and photosynthesis at the leaf level, which is confirmed by active fluorescence measurements.

We propose to use a two-big-leaf LUE model instead of the commonly used one-big-leaf LUE model for interpreting the SIF-GPP relationship. This is because of clearly different relationships between fluorescence emission and photochemical light use efficiencies for sunlit and shaded leaves. The use of the two-big-leaf LUE model leads to a better understanding of the SIF-GPP relationship and its responses to weather conditions, such as clouds and fraction of diffuse light, as well as its responses to canopy structure, such as canopy openness and growth stages.

We also confirm that heat dissipation is responsible for the positive relationship between the efficiencies of fluorescence and photochemistry. Sustained (i.e., diurnally stable) heat dissipation increased through the crop's growth into the senescent stage, which caused the late season decrease in photosynthetic light use efficiency. The seasonal variation in sustained heat dissipation contributed to a moderate positive relationship between the efficiencies of fluorescence and photochemistry at the seasonal scale. At the diurnal scale, the reversible heat dissipation is responsible for the change of photosynthetic light use efficiency.

Author contributions: P.Y., E.M., C.vdT and P.C. designed and performed research; P.Y. analyzed the data and prepared the original draft; P.Y., E.M., C.vdT and P.C. reviewed and edited the paper.

Data availability: The data is provided as a supplement.

Competing interests: The authors declare no conflict of interest.

Acknowledgements

This work was supported by the Netherlands Organization for Scientific Research, grant ALWGO.2017.018. The collection of field data and the work of co-authors Campbell and Middleton were supported by NASA's Terrestrial Ecology program grant 80NSSC19M0110, Land Cover Land Use Change grant 80NSSC18K0337, and the Biospherc-Sciences Laboratory at NASA Goddard Space Flight Center.

https://doi.org/10.5194/bg-2020-323
Preprint. Discussion started: 8 September 2020

References

Baba, K., Shibata, R. and Sibuya, M.: Partial correlation and conditional correlation as measures of conditional independence, Aust. New Zeal. J. Stat., 46(4), 657–664, doi:10.1111/j.1467-842X.2004.00360.x, 2004.

Baker, N. R.: Chlorophyll fluorescence: A probe of photosynthesis in vivo, Annu. Rev. Plant Biol., 59, 89–113, doi:10.1146/annurev.arplant.59.032607.092759, 2008.

Campbell, P. K. E., Huemmrich, K. F., Middleton, E. M., Ward, L. A., Julitta, T., Daughtry, C. S. T., Burkart, A., Russ, A. L. and Kustas, W. P.: Diurnal and seasonal variations in chlorophyll fluorescence associated with photosynthesis at leaf and canopy scales, Remote Sens., 11(5), 488, doi:10.3390/rs11050488, 2019.

Cogliati, S., Verhoef, W., Kraft, S., Sabater, N., Alonso, L., Vicent, J., Moreno, J., Drusch, M. and Colombo, R.: Retrieval of sun-induced fluorescence using advanced spectral fitting methods, Remote Sens. Environ., 169, 344–357, doi:10.1016/j.rse.2015.08.022, 2015.

Collatz, G.: Coupled Photosynthesis-Stomatal Conductance Model for Leaves of C4 Plants, Aust. J. Plant Physiol., 19(5), 1992.

Collatz, G. J., Ball, J. T., Grivet, C. and Berry, J. A.: Physiological and environmental regulation of stomatal conductance, photosynthesis and transpiration: a model that includes a laminar boundary layer, Agric. For. Meteorol., 54(2–4), 107–136, doi:10.1016/0168-1923(91)90002-8, 1991.

Dai, Y., Dickinson, R. E. and Wang, Y. P.: A two-big-leaf model for canopy temperature, photosynthesis, and stomatal conductance, J. Clim., 17(12), 2281–2299, doi:10.1175/1520-0442(2004)017<2281:ATMFCT>2.0.CO;2, 2004.

Damm, A., Guanter, L., Paul-Limoges, E., van der Tol, C., Hueni, A., Buchmann, N., Eugster, W., Ammann, C. and Schaepman, M. E.: Far-red sun-induced chlorophyll fluorescence shows ecosystem-specific relationships to gross primary production: An assessment based on observational and modeling approaches, Remote Sens. Environ., 166, 91–105, doi:10.1016/j.rse.2015.06.004, 2015.

Dechant, B., Ryu, Y., Badgley, G., Zeng, Y., Berry, J. A., Zhang, Y., Goulas, Y., Li, Z., Zhang, Q., Kang, M., Li, J. and Moya, I.: Canopy structure explains the relationship between photosynthesis and sun-induced chlorophyll fluorescence in crops, Remote Sens. Environ., 241, 111733, doi:10.1016/j.rse.2020.111733, 2020.

Friend, A. D.: Modelling canopy CO2 fluxes: Are “big-leaf” simplifications justified?, Glob. Ecol. Biogeogr., 10(6), 603–619, doi:10.1046/j.1466-822X.2001.00268.x, 2001.

Gamon, J. A., Peñuelas, J. and Field, C. B.: A narrow-waveband spectral index that tracks diurnal changes in photosynthetic efficiency, Remote Sens. Environ., 41(1), 35–44, doi:10.1016/0034-4257(92)90059-S, 1992.

Garbulsky, M. F., Peñuelas, J., Gamon, J., Inoue, Y. and Filella, I.: The photochemical reflectance index (PRI) and the remote sensing of leaf, canopy and ecosystem radiation use efficiencies. A review and meta-analysis, Remote Sens. Environ., 115(2), 281–297, doi:10.1016/j.rse.2010.08.023, 2011.

Genty, B., Briantais, J. M. and Baker, N. R.: The relationship between the quantum yield of photosynthetic electron transport

and quenching of chlorophyll fluorescence, Biochim. Biophys. Acta - Gen. Subj., 990(1), 87–92, doi:10.1016/S0304-4165(89)80016-9, 1989.

Givnish, T. J.: Adaptation to sun and shade: a whole-plant perspective, Aust. J. Plant Physiol., 15(1–2), 63–92, doi:10.1071/pp9880063, 1988.

Gu, L., Han, J., Wood, J. D., Chang, C. Y. Y. and Sun, Y.: Sun-induced Chl fluorescence and its importance for biophysical modeling of photosynthesis based on light reactions, New Phytol., 223(3), 1179–1191, doi:10.1111/nph.15796, 2019.

Guan, K., Berry, J. A., Zhang, Y., Joiner, J., Guanter, L., Badgley, G. and Lobell, D. B.: Improving the monitoring of crop productivity using spaceborne solar-induced fluorescence, Glob. Chang. Biol., 22(2), 716–726, doi:10.1111/gcb.13136, 2016.

Guanter, L., Zhang, Y., Jung, M., Joiner, J., Voigt, M., Berry, J. A., Frankenberg, C., Huete, A. R., Zarco-Tejada, P., Lee, J. E., Moran, M. S., Ponce-Campos, G., Beer, C., Camps-Valls, G., Buchmann, N., Gianelle, D., Klumpp, K., Cescatti, A., Baker, J. M. and Griffis, T. J.: Global and time-resolved monitoring of crop photosynthesis with chlorophyll fluorescence, Proc. Natl. Acad. Sci. U. S. A., 111(14), E1327–E1333, doi:10.1073/pnas.1320008111, 2014.

He, L., Chen, J. M., Liu, J., Mo, G. and Joiner, J.: Angular normalization of GOME-2 Sun-induced chlorophyll fluorescence observation as a better proxy of vegetation productivity, Geophys. Res. Lett., 44(11), 5691–5699, doi:10.1002/2017GL073708, 2017.

Heber, U., Lange, O. L. and Shuvalov, V. A.: Conservation and dissipation of light energy as complementary processes: Homoiohydric and poikilohydric autotrophs, J. Exp. Bot., 57(6), 1211–1223, doi:10.1093/jxb/erj104, 2006.

Hendrickson, L., Furbank, R. T. and Chow, W. S.: A simple alternative approach to assessing the fate of absorbed light energy using chlorophyll fluorescence, Photosynth. Res., 82(1), 73–81, doi:10.1023/B:PRES.0000040446.87305.f4, 2004.

Hilker, T., Lyapustin, A., Hall, F. G., Wang, Y., Coops, N. C., Drolet, G. and Black, T. A.: An assessment of photosynthetic light use efficiency from space: Modeling the atmospheric and directional impacts on PRI reflectance, Remote Sens. Environ., 113(11), 2463–2475, doi:10.1016/j.rse.2009.07.012, 2009.

Huete, A., Didan, K., Miura, T., Rodriguez, E. P., Gao, X. and Ferreira, L. G.: Overview of the radiometric and biophysical performance of the MODIS vegetation indices, Remote Sens. Environ., 83(1–2), 195–213, doi:10.1016/S0034-4257(02)00096-2, 2002.

Jackson, L. W. R.: Effect of Shade on Leaf Structure of Deciduous Tree Species, Ecology, 48(3), 498–499, doi:10.2307/1932686, 1967.

Köhler, P., Guanter, L., Kobayashi, H., Walther, S. and Yang, W.: Assessing the potential of sun-induced fluorescence and the canopy scattering coefficient to track large-scale vegetation dynamics in Amazon forests, Remote Sens. Environ., 204, 769–785, doi:10.1016/j.rse.2017.09.025, 2018.

de la Fuente, A., Bing, N., Hoeschele, I. and Mendes, P.: Discovery of meaningful associations in genomic data using partial correlation coefficients, Bioinformatics, 20(18), 3565–3574, doi:10.1093/bioinformatics/bth445, 2004.

De Lannoy, G. J. M., Verhoest, N. E. C., Houser, P. R., Gish, T. J. and Van Meirvenne, M.: Spatial and temporal characteristics of soil moisture in an intensively monitored agricultural field (OPE3), J. Hydrol., 331(3–4), 719–730,

doi:10.1016/j.jhydrol.2006.06.016, 2006.

Luo, X., Chen, J. M., Liu, J., Black, T. A., Croft, H., Staebler, R., He, L., Arain, M. A., Chen, B., Mo, G., Gonsamo, A. and McCaughey, H.: Comparison of Big-Leaf, Two-Big-Leaf, and Two-Leaf Upscaling Schemes for Evapotranspiration Estimation Using Coupled Carbon-Water Modeling, J. Geophys. Res. Biogeosciences, 123(1), 207–225, doi:10.1002/2017JG003978, 2018.

Magney, T. S., Bowling, D. R., Logan, B. A., Grossmann, K., Stutz, J., Blanken, P. D., Burns, S. P., Cheng, R., Garcia, M. A., Köhler, P., Lopez, S., Parazoo, N. C., Raczka, B., Schimel, D. and Frankenberg, C.: Mechanistic evidence for tracking the seasonality of photosynthesis with solar-induced fluorescence, Proc. Natl. Acad. Sci. U. S. A., 116(24), 11640–11645, doi:10.1073/pnas.1900278116, 2019.

Maxwell, K. and Johnson, G. N.: Chlorophyll fluorescence—a practical guide, J. Exp. Bot., 51(345), 659–668, 2000.

Miao, G., Guan, K., Yang, X., Bernacchi, C. J., Berry, J. A., DeLucia, E. H., Wu, J., Moore, C. E., Meacham, K., Cai, Y., Peng, B., Kimm, H. and Masters, M. D.: Sun-Induced Chlorophyll Fluorescence, Photosynthesis, and Light Use Efficiency of a Soybean Field from Seasonally Continuous Measurements, J. Geophys. Res. Biogeosciences, 123(2), 610–623, doi:10.1002/2017JG004180, 2018.

Middleton, E. M., Cheng, Y. Ben, Hilker, T., Black, T. A., Krishnan, P., Coops, N. C. and Huemmrich, K. F.: Linking foliage spectral responses to canopy-level ecosystem photosynthetic light-use efficiency at a douglas-fir forest in canada, Can. J. Remote Sens., 35(2), 166–188, doi:10.5589/m09-008, 2009.

Middleton, E. M., Huemmrich, K. F., Landis, D. R., Black, T. A., Barr, A. G. and McCaughey, J. H.: Photosynthetic efficiency of northern forest ecosystems using a MODIS-derived Photochemical Reflectance Index (PRI), Remote Sens. Environ., 187, 345–366, doi:10.1016/j.rse.2016.10.021, 2016.

Middleton, E. M., Huemmrich, K. F., Zhang, Q., Campbell, P. K. E. and Landis, D. R.: Photosynthetic Efficiency and Vegetation Stress, Biophys. Biochem. Charact. Plant Species Stud., 133–179, doi:10.1201/9780429431180-5, 2019.

Migliavacca, M., Perez-Priego, O., Rossini, M., El-Madany, T. S., Moreno, G., van der Tol, C., Rascher, U., Berninger, A., Bessenbacher, V., Burkart, A., Carrara, A., Fava, F., Guan, J. H., Hammer, T. W., Henkel, K., Juarez-Alcalde, E., Julitta, T., Kolle, O., Martín, M. P., Musavi, T., Pacheco-Labrador, J., Pérez-Burgueño, A., Wutzler, T., Zaehle, S. and Reichstein, M.: Plant functional traits and canopy structure control the relationship between photosynthetic CO2 uptake and far-red sun-induced fluorescence in a Mediterranean grassland under different nutrient availability, New Phytol., 214(3), 1078–1091, doi:10.1111/nph.14437, 2017.

Mohammed, G. H., Colombo, R., Middleton, E. M., Rascher, U., van der Tol, C., Nedbal, L., Goulas, Y., Pérez-Priego, O., Damm, A., Meroni, M., Joiner, J., Cogliati, S., Verhoef, W., Malenovský, Z., Gastellu-Etchegorry, J. P., Miller, J. R., Guanter, L., Moreno, J., Moya, I., Berry, J. A., Frankenberg, C. and Zarco-Tejada, P. J.: Remote sensing of solar-induced chlorophyll fluorescence (SIF) in vegetation: 50 years of progress, Remote Sens. Environ., 231, 111177, doi:10.1016/j.rse.2019.04.030, 2019.

Monteith, J. L.: Climate and the efficiency of crop production in Britain, Philos. Trans. R. Soc. London. B, Biol. Sci., 281(980),

277–294, doi:10.1098/rstb.1977.0140, 1977.

Müller, P., Li, X. P. and Niyogi, K. K.: Non-photochemical quenching. A response to excess light energy, Plant Physiol., 125(4), 1558–1566, doi:10.1104/pp.125.4.1558, 2001.

Porcar-Castell, A., Pfündel, E., Korhonen, J. F. J. and Juurola, E.: A new monitoring PAM fluorometer (MONI-PAM) to study the short- and long-term acclimation of photosystem II in field conditions, Photosynth. Res., 96(2), 173–179, doi:10.1007/s11120-008-9292-3, 2008.

Porcar-Castell, A., Tyystjärvi, E., Atherton, J., Van Der Tol, C., Flexas, J., Pfündel, E. E., Moreno, J., Frankenberg, C. and Berry, J. A.: Linking chlorophyll a fluorescence to photosynthesis for remote sensing applications: Mechanisms and challenges, J. Exp. Bot., 65(15), 4065–4095, doi:10.1093/jxb/eru191, 2014.

Qiu, B., Chen, J. M., Ju, W., Zhang, Q. and Zhang, Y.: Simulating emission and scattering of solar-induced chlorophyll fluorescence at far-red band in global vegetation with different canopy structures, Remote Sens. Environ., 233, 111373, doi:10.1016/j.rse.2019.111373, 2019.

Reichstein, M., Falge, E., Baldocchi, D., Papale, D., Aubinet, M., Berbigier, P., Bernhofer, C., Buchmann, N., Gilmanov, T., Granier, A., Grünwald, T., Havránková, K., Ilvesniemi, H., Janous, D., Knohl, A., Laurila, T., Lohila, A., Loustau, D., Matteucci, G., Meyers, T., Miglietta, F., Ourcival, J. M., Pumpanen, J., Rambal, S., Rotenberg, E., Sanz, M., Tenhunen, J., Seufert, G., Vaccari, F., Vesala, T., Yakir, D. and Valentini, R.: On the separation of net ecosystem exchange into assimilation and ecosystem respiration: Review and improved algorithm, Glob. Chang. Biol., 11(9), 1424–1439, doi:10.1111/j.1365-2486.2005.001002.x, 2005.

Rosema, A., Verhoef, W., Schroote, J. and Snel, J. F. H.: Simulating fluorescence light-canopy interaction in support of laser-induced fluorescence measurements, Remote Sens. Environ., 37(2), 117–130, doi:10.1016/0034-4257(91)90023-Y, 1991.

Rossini, M., Meroni, M., Migliavacca, M., Manca, G., Cogliati, S., Busetto, L., Picchi, V., Cescatti, A., Seufert, G. and Colombo, R.: High resolution field spectroscopy measurements for estimating gross ecosystem production in a rice field, Agric. For. Meteorol., 150(9), 1283–1296, doi:10.1016/j.agrformet.2010.05.011, 2010.

Ryu, Y., Berry, J. A. and Baldocchi, D. D.: What is global photosynthesis? History, uncertainties and opportunities, Remote Sens. Environ., 223(January), 95–114, doi:10.1016/j.rse.2019.01.016, 2019.

Schreiber, U., Schliwa, U. and Bilger, W.: Continuous recording of photochemical and non-photochemical chlorophyll fluorescence quenching with a new type of modulation fluorometer, Photosynth. Res., 10(1–2), 51–62, doi:10.1007/BF00024185, 1986.

Stenberg, P. and Manninen, T.: The effect of clumping on canopy scattering and its directional properties: a model simulation using spectral invariants, Int. J. Remote Sens., 36(19–20), 5178–5191, doi:10.1080/01431161.2015.1049383, 2015.

Van Der Tol, C., Verhoef, W., Timmermans, J., Verhoef, A. and Su, Z.: An integrated model of soil-canopy spectral radiances, photosynthesis, fluorescence, temperature and energy balance, Biogeosciences, 6(12), 3109–3129, doi:10.5194/bg-6-3109-2009, 2009.

Van Der Tol, C., Berry, J. A., Campbell, P. K. E. and Rascher, U.: Models of fluorescence and photosynthesis for interpreting

https://doi.org/10.5194/bg-2020-323
Preprint. Discussion started: 8 September 2020

measurements of solar-induced chlorophyll fluorescence, J. Geophys. Res. Biogeosciences, 119(12), 2312–2327, doi:10.1002/2014JG002713, 2014.

Verhoef, W.: Light scattering by leaf layers with application to canopy reflectance modeling: The SAIL model, Remote Sens. Environ., 16(2), 125–141, doi:10.1016/0034-4257(84)90057-9, 1984.

Vilfan, N., Van der Tol, C., Yang, P., Wyber, R., Malenovský, Z., Robinson, S. A. and Verhoef, W.: Extending Fluspect to simulate xanthophyll driven leaf reflectance dynamics, Remote Sens. Environ., 211(March), 345–356, doi:10.1016/j.rse.2018.04.012, 2018.

Viña, A. and Gitelson, A. A.: New developments in the remote estimation of the fraction of absorbed photosynthetically active radiation in crops, Geophys. Res. Lett., 32(17), 1–4, doi:10.1029/2005GL023647, 2005.

Wang, Y. P. and Leuning, R.: A two-leaf model for canopy conductance, photosynthesis and partitioning of available energy I: Model description and comparison with a multi-layered model, Agric. For. Meteorol., 91(1–2), 89–111, doi:10.1016/S0168-1923(98)00061-6, 1998.

Wieneke, S., Ahrends, H., Damm, A., Pinto, F., Stadler, A., Rossini, M. and Rascher, U.: Airborne based spectroscopy of red and far-red sun-induced chlorophyll fluorescence: Implications for improved estimates of gross primary productivity, Remote Sens. Environ., 184, 654–667, doi:10.1016/j.rse.2016.07.025, 2016.

Xiao, X., Zhang, Q., Braswell, B., Urbanski, S., Boles, S., Wofsy, S., Moore, B. and Ojima, D.: Modeling gross primary production of temperate deciduous broadleaf forest using satellite images and climate data, Remote Sens. Environ., 91(2), 256–270, doi:10.1016/j.rse.2004.03.010, 2004.

Yang, K., Ryu, Y., Dechant, B., Berry, J. A., Hwang, Y., Jiang, C., Kang, M., Kim, J., Kimm, H., Kornfeld, A. and Yang, X.: Sun-induced chlorophyll fluorescence is more strongly related to absorbed light than to photosynthesis at half-hourly resolution in a rice paddy, Remote Sens. Environ., 216, 658–673, doi:10.1016/j.rse.2018.07.008, 2018.

Yang, P. and Van der Tol, C.: Linking canopy scattering of far-red sun-induced chlorophyll fluorescence with reflectance, Remote Sens. Environ., 209(October 2017), 456–467, doi:10.1016/j.rse.2018.02.029, 2018.

Yang, P., van der Tol, C., Campbell, P. K. E. and Middleton, E. M.: Fluorescence Correction Vegetation Index (FCVI): A physically based reflectance index to separate physiological and non-physiological information in far-red sun-induced chlorophyll fluorescence, Remote Sens. Environ., 240, 111676, doi:10.1016/j.rse.2020.111676, 2020.

Yang, X., Tang, J., Mustard, J. F., Lee, J. E., Rossini, M., Joiner, J., Munger, J. W., Kornfeld, A. and Richardson, A. D.: Solar-induced chlorophyll fluorescence that correlates with canopy photosynthesis on diurnal and seasonal scales in a temperate deciduous forest, Geophys. Res. Lett., 42(8), 2977–2987, doi:10.1002/2015GL063201, 2015.

Zhang, Q., M. Chen, J., Ju, W., Wang, H., Qiu, F., Yang, F., Fan, W., Huang, Q., Wang, Y. ping, Feng, Y., Wang, X. and Zhang, F.: Improving the ability of the photochemical reflectance index to track canopy light use efficiency through differentiating sunlit and shaded leaves, Remote Sens. Environ., 194, 1–15, doi:10.1016/j.rse.2017.03.012, 2017.

Zhang, Y., Guanter, L., Berry, J. A., Joiner, J., van der Tol, C., Huete, A., Gitelson, A., Voigt, M. and Köhler, P.: Estimation of vegetation photosynthetic capacity from space-based measurements of chlorophyll fluorescence for terrestrial biosphere

https://doi.org/10.5194/bg-2020-323
Preprint. Discussion started: 8 September 2020

models, Glob. Chang. Biol., 20(12), 3727–3742, doi:10.1111/gcb.12664, 2014.

Zhu, X. G., Long, S. P. and Ort, D. R.: What is the maximum efficiency with which photosynthesis can convert solar energy into biomass?, Curr. Opin. Biotechnol., 19(2), 153–159, doi:10.1016/j.copbio.2008.02.004, 2008.

Tables and figures

Table 1: Summary of the main canopy and leaf field measurements used in the analyses.

	Variable	Description	Measuring system	Unit	Temporal resolution
Canopy	GPP	gross primary production	eddy covariance system	mg m^{-2} s^{-1}	30 minutes
	F_{760}	canopy SIF at 760nm	QEpro (in FLOX)	mW m^{-2} s^{-1}	1-3 minutes
	$iPAR_{canopy}$	TOC incoming PAR	FLAME-S (in FLOX)	μmol m^{-2} s^{-1}	1-3 minutes
	$fAPAR_{canopy}$	canopy fraction of absorbed PAR	FLAME-S (in FLOX)	-	1-3 minutes
Leaf	$iPAR_{leaf}$	leaf incoming PAR	MONIPAM system	μmol m^{-2} s^{-1}	10 minutes
	$fAPAR_{leaf}$	leaf fAPAR	ASD spectrometer	-	-
	F_m	maximal fluorescence levels	MONIPAM system	-	10 minutes
	F_s	steady-state fluorescence levels	MONIPAM system	-	10 minutes

Table 2: Correlation coefficients and partial correlation coefficients (i.e. controlling for or eliminating separate effects) between fluorescence and photosynthesis.

Φ_F^* vs. Φ_P	Sunlit leaves	Shaded leaves
Without controls	0.53	0.10
Controlling Φ_N	0.05	-0.31
Controlling Φ_D	0.08	-0.35
Controlling both Φ_N and Φ_D	-0.75	-0.75

https://doi.org/10.5194/bg-2020-323
Preprint. Discussion started: 8 September 2020

Biogeosciences Discussions
Open Access
EGU

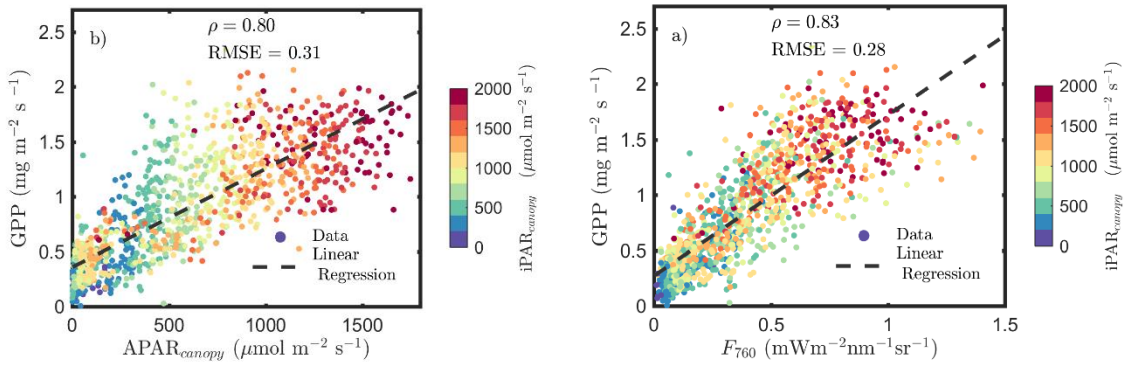

Figure 1: Relationships between far-red SIF (F_{760}) and GPP, and between APAR$_{canopy}$ and GPP of a corn canopy in the 2017 growing season with half-hour temporal resolution during daylight hours. F_{760} and APAR$_{canopy}$ were retrieved from FLoX canopy measurements. GPP was obtained from the site's flux tower measurements.

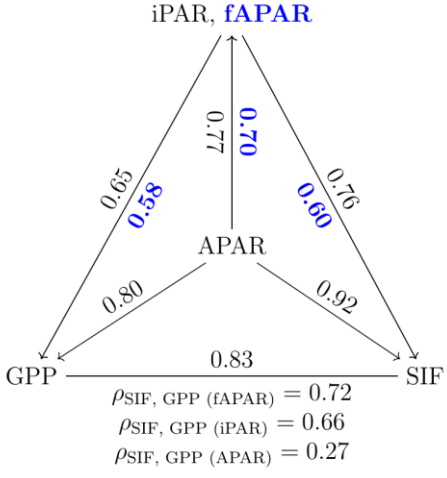

Figure 2: Pearson correlation coefficients among the canopy variables iPAR$_{canopy}$, APAR$_{canopy}$, fAPAR$_{canopy}$ (indicated in bold, blue text), GPP, and SIF for a corn canopy across the 2017 growing season. The partial correlation coefficients between SIF and GPP (listed at the base of the triangle) were determined by removing the effects of the controlling variables, fAPAR, iPAR and APAR, respectively. Measurements had a half-hour resolution.

https://doi.org/10.5194/bg-2020-323
Preprint. Discussion started: 8 September 2020

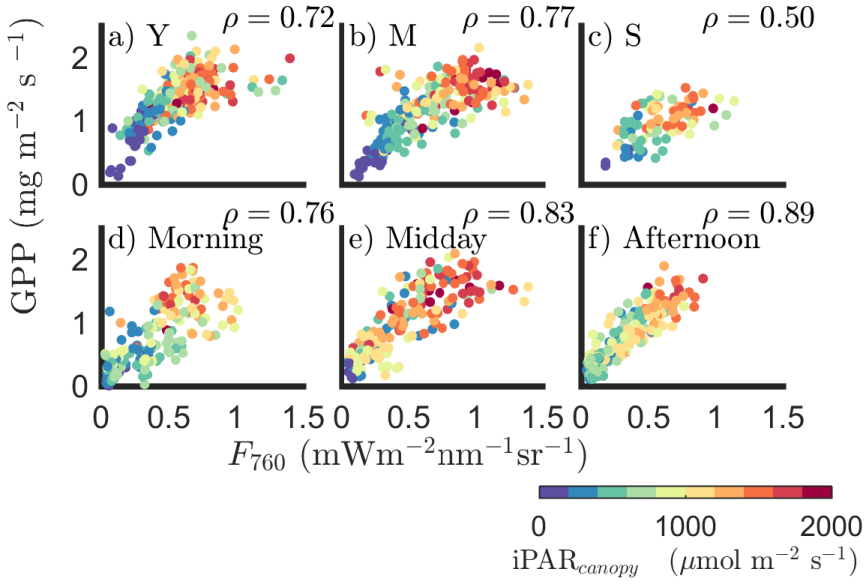

Figure 3: Relationships between far-red SIF (F_{760}) and GPP of a corn canopy in the 2017 growing season with half-hour temporal resolution during daylight hours for three growth stages (a-c):young (Y), mature (M) and senescent (S); for three times of a day (d-f): morning (9:00-11:00), midday (11:00-14:00) and afternoon (14:00-17:00).

https://doi.org/10.5194/bg-2020-323
Preprint. Discussion started: 8 September 2020

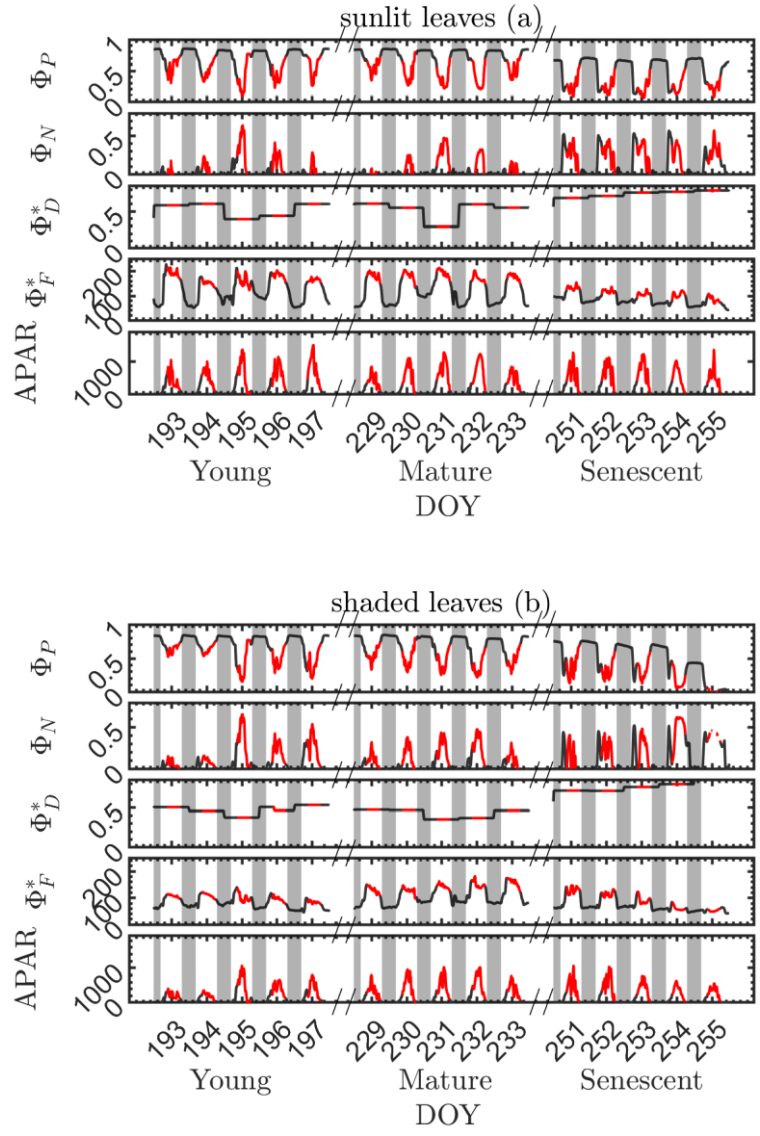

Figure 4: Photosystem energy partitioning obtained from *in situ* active fluorescence measurements made on individual leaves of a corn canopy during the 2017 growing season. Shown are the absolute light use efficiency of photochemistry (Φ_P), the reversible heat dissipation (Φ_N), the relative light use efficiency of sustained heat dissipation (Φ_D^*), the relative light use efficiency of fluorescence (Φ_F^*) and the photosynthetically active radiation absorbed by individually leaves ($APAR_{leaf}$, µmol m^{-2} s^{-1}) for sunlit leaves (a) and shaded leaves (b). The nighttime periods from sunset to sunrise of the next day are marked with grey rectangles and the daylight measurements from 9:00 to 17:00 are indicated with red tracks.

https://doi.org/10.5194/bg-2020-323
Preprint. Discussion started: 8 September 2020

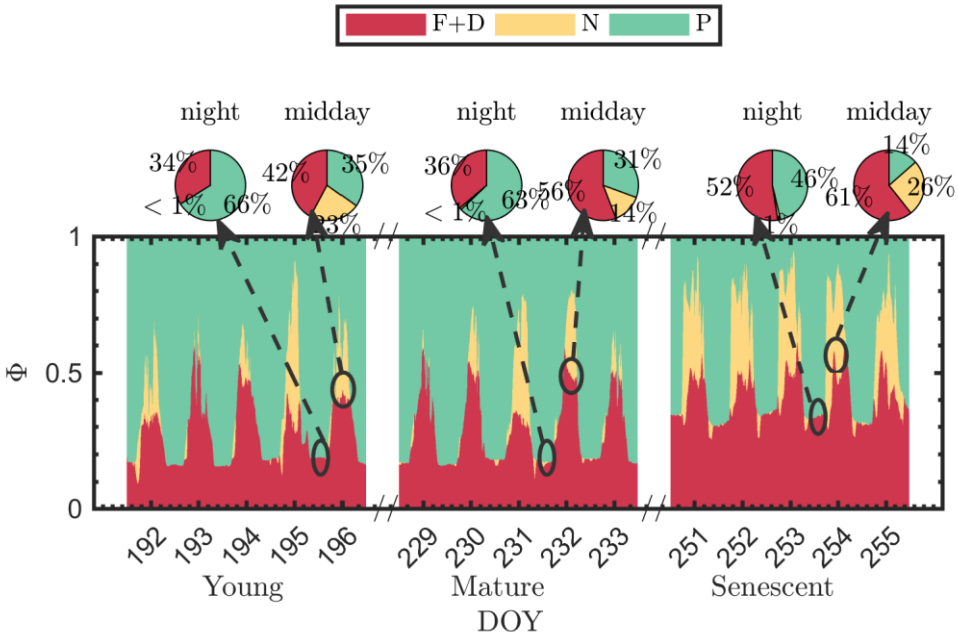

Figure 5: Summary chart of the efficiency responses presented in Fig. 4. The energy partitioning in both nighttime (sunset - sunrise) and midday (11:00 - 14:00) for one representative date per growth stage (Y, DOY 194; M, DOY 232; and S, DOY 254) is diagrammed in the pie charts.

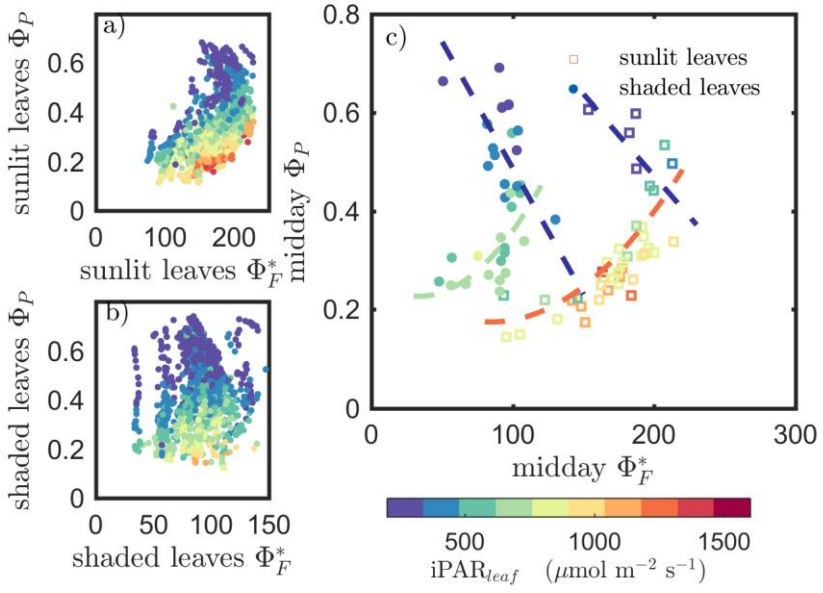

https://doi.org/10.5194/bg-2020-323
Preprint. Discussion started: 8 September 2020

Biogeosciences Discussions
Open Access
EGU

Figure 6: Relationships between daylight measurements (9:00 - 17:00, a and b), and seasonally midday-averaged (11:00 - 14:00, c) of light use efficiency of photochemistry (Φ_P) and relative fluorescence light emission efficiency (Φ_F^*) for sunlit leaves and shaded leaves across the 2017 growing season in a corn canopy. The data in c) were classified in two groups by $iPAR_{leaf}$ with a threshold value of 500 µmol m^{-2} s^{-1}.

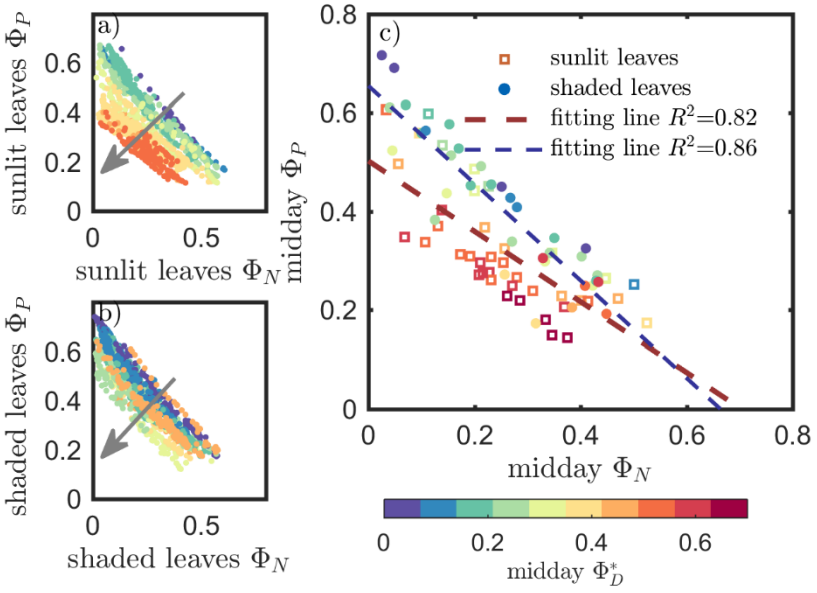

Figure 7: Relationships between daylight measurements (9:00 - 17:00, a and b), and seasonally midday-averaged (11:00 - 14:00, c) of light use efficiencies of photochemistry (Φ_P) and reversible heat dissipation (Φ_N) showing the change in the relative light use efficiency of sustained heat dissipation (Φ_D^*) for sunlit leaves (a) and shaded leaves (b). The arrows indicate the shift in linear response between Φ_P and Φ_N as Φ_D^* becomes the dominant energy pathway, thus lowering the photosynthetic potential.

https://doi.org/10.5194/bg-2020-323
Preprint. Discussion started: 8 September 2020

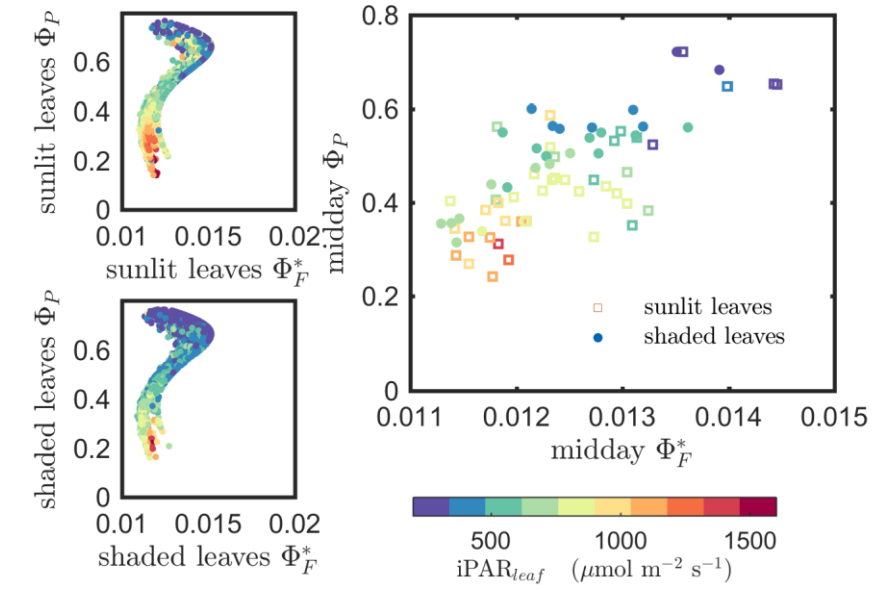

Figure 8: Reproduction of Fig. 6 with simulated variables from the biochemical model of Van der Tol et al. (2014).

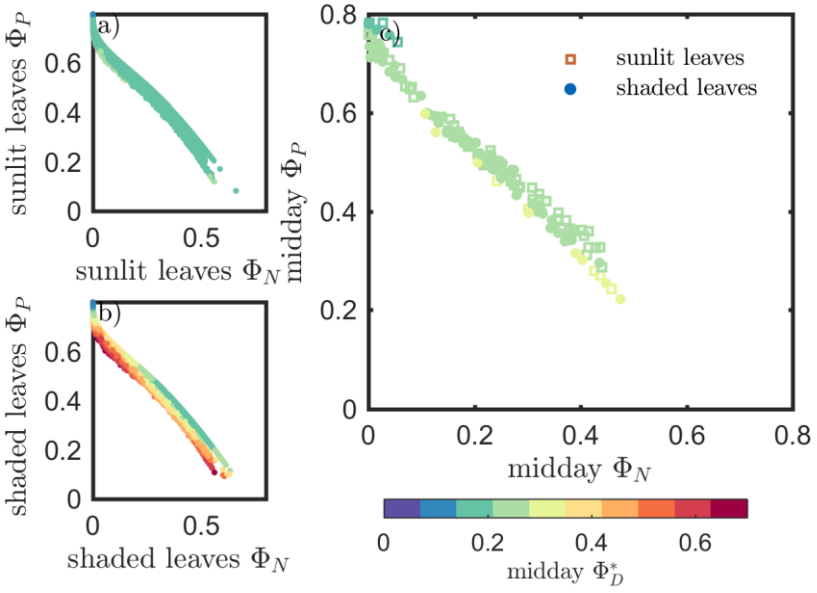

Figure 9: Reproduction of Fig. 7 with simulated variables from the biochemical model of Van der Tol et al. (2014).

https://doi.org/10.5194/bg-2020-323
Preprint. Discussion started: 8 September 2020

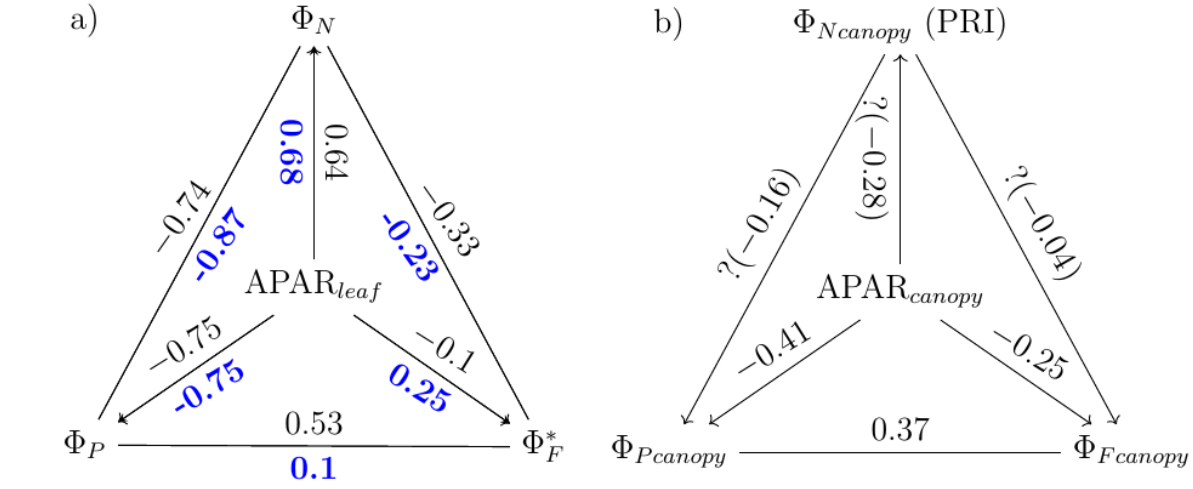

Figure 10: Pearson correlation coefficients between absorbed PAR (APAR$_{leaf}$ and APAR$_{canopy}$), and light use efficiencies for a corn canopy across the 2017 growing season at both leaf (a) and canopy levels (b). Light use efficiency of photochemistry (Φ_P), relative fluorescence emission efficiency (Φ_F^*), and efficiency of variable heat dissipation (Φ_N) of sunlit leaves and shaded leaves (indicated in bold, blue text) during daytime (9:00 to 17:00) are obtained from *in situ* active fluorescence measurements made on individual leaves. Canopy light use efficiency of photochemistry ($\Phi_{Pcanopy}$) and of fluorescence ($\Phi_{Fcanopy}$) are approximated by GPP/APAR$_{canopy}$ and F_{760}/APAR$_{canopy}$ respectively. PRI is used as an indicator of canopy light use efficiency of variable heat dissipation ($\Phi_{Ncanopy}$), but the exact values of $\Phi_{Fcanopy}$ are unknown (noted with "?" markers). The leaf-level and canopy-level variables had 10-minute and half-hour resolutions, respectively.

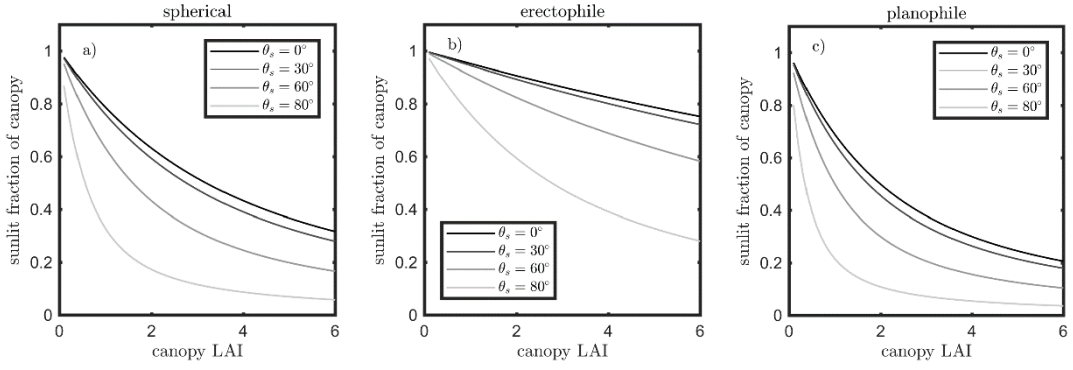

Figure 11: Fraction of sunlit canopy changing with canopy LAI and solar zenith angle (θ_s) for canopy with spherical (a), erectophile (b) and planophile (c).